KERNFORSCHUNGSANLAGE JÜLICH GmbH
Institut für Festkörperforschung

Crystal Structure Investigations on Cation-Substituted Alums by X-Ray and Neutron Diffraction

by

A. M. Abdeen

Jül - 1653
April 1980
ISSN 0366-0885

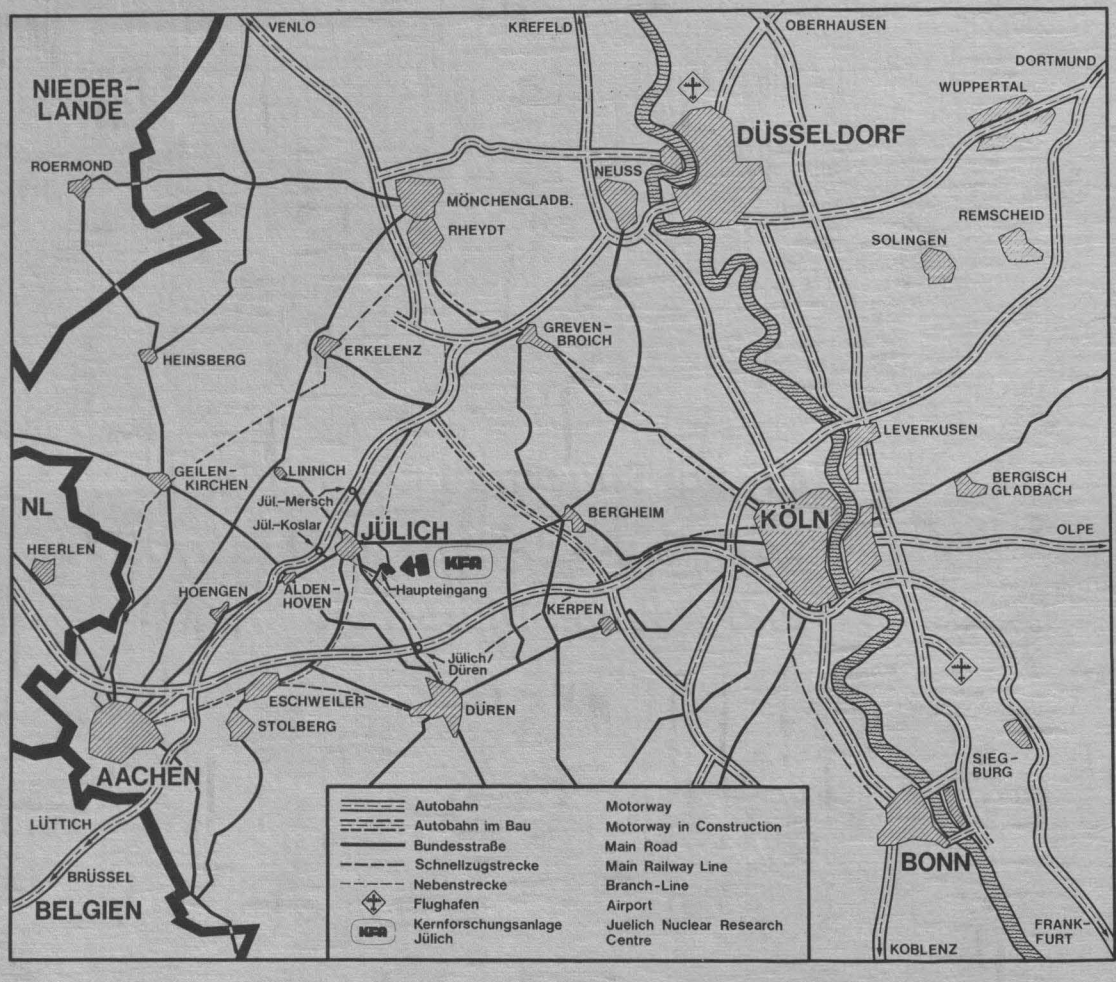

Als Manuskript gedruckt

Berichte der Kernforschungsanlage Jülich - Nr. 1653

Institut für Festkörperforschung Jül - 1653

Zu beziehen durch: ZENTRALBIBLIOTHEK der Kernforschungsanlage Jülich GmbH

Postfach 1913 · D-5170 Jülich (Bundesrepublik Deutschland)

Telefon: 02461/611 · Telex: 833556 kfa d

Crystal Structure Investigations on Cation-Substituted Alums by X-Ray and Neutron Diffraction

Mitteilung aus dem Mineralogischen Institut
der Universität Bonn in Zusammenarbeit mit dem Institut
für Festkörperforschung der KFA Jülich

by

A. M. Abdeen

D 5 (Diss. Uni. Bonn)

ACKNOWLEDGEMENTS

I would like to express my deep appreciation to Prof. Dr. G. Will for suggesting this research problem and for his valuable supervision and help throughout the course of this work.

I am also indepted to Prof. Dr. K. Recker, Prof. Dr. A. Weiss and Dr. N. Weiden for providing the single crystals and to Prof. Dr. N. Barakat, the cultural counsellor in Bonn, for his continuous interest in this work.

I want to express my sincere gratitude to Dr. W. Schäfer for his continuous assistance and valuable guidance throughout this work. Thanks are also due to Dr. A. Kirfel and Dr. M.O. Bargouth for helpful discussions and to Mr. R. Skowronek for technical assistance.

The financial support of the Bundesministerium für Forschung und Technologie for providing the neutron diffractometer is gratefully acknowledged.

Finally I would like to thank Tanta University, Egypt for award of a student fellow ship.

Abstract

The crystal structures of the three alums: $NH_4Al(SO_4)_2.12H_2O$, $(NH_3CH_3)Al(SO_4)_2.12H_2O$ and $(NH_3OH)Al(SO_4)_2.12H_2O$ have been determined from three-dimensional neutron diffraction data enhanced by X-ray diffraction when necessary. These compounds crystallize cubic in space group Pa3.

The structures of the three alums exhibit partial occupancies of crystallographic sites for the NH_4, (NH_3CH_3) and (NH_3OH) group atoms. This can be explained by a quantized rotation of the three groups around an axis perpendicular to the [111] direction.

Some of the $(SO_4)^{2-}$ groups in the NH_4-alum are disordered with about 17% of the sulfate tetrahedra being in a reversed orientation around the sulfur atom. The disorder in (NH_3CH_3) and (NH_3OH)-alums is only 4,3% and 3.0% respectively.

The atoms in the alum structures are held together by a system of hydrogen bonds between the water molecules and between the water molecules and the sulfate oxygen atoms. In these three structures there is a strong indication that shorter hydrogen bonds tend to be nearly linear.

CONTENTS

1. INTRODUCTION

The goal of this thesis was the precise structure determination of the three alums: $NH_4Al(SO_4)_2.12H_2O$, $(NH_3CH_3)Al(SO_4)_2.12H_2O$ and $(NH_3OH)Al(SO_4)_2.12H_2O$ by neutron diffraction enhanced by X-ray diffraction when necessary. Neutron diffraction is sensitive to hydrogen and allows therefore the precise localization of hydrogen atoms in a crystal. A detailed description of the goals of this thesis is given at the end of this section, first a general introduction to the alums and a short review of previous investigations shall be given.

The alums form a series of double salt crystals with the general formula $M^+T^{3+}(RO_4)_2.12H_2O$, where M^+ represents a monovalent metal such as Na, K, Rb, Cs or a group such as NH_4, NH_3CH_3 or NH_3OH. T^{3+} represents a trivalent metal such as Al, V, Cr, Fe, Ga or In and R stands for S, Se or Te. BeF_4^{2-} alums are also known. The number of possible salts is therefore large, but comprehensive diffraction analysis have been carried out for only a few of them.

The physical properties of the alums have been extensively studied by a great variety of experimental methods like optical absorption measurements /1,2/, specific heat measurements /3,4/, measurements of the elastic constants /5,6/, of piezooptical constants /7/, of electrogyration effects /8,9/, of dielectric properties /10-13/. A review of the physical properties of various chromium alums for example has been published by Eisenstein /14/.

A large number of alums undergo a transtion into a ferroelectric phase at low temperature, first identified by Pepinsky et al. /15/ in (NH_3CH_3) aluminium and (NH_2CONH_2) chromium alums and later in other ammonium and ammonium-substituted alums /16/.

A variety of spectroscopic methods has been applied to study the ferroelectric transformations of the alums, specially nuclear magnetic resonance and Mössbauer spectroscopy. Proton magnetic resonance was applied to study methylammonium alum /17-19/ and others /19-21/, the ^{27}Al-nuclear magnetic resonance spectroscopy for the study of $NH_4Al(SO_4)_2.12H_2O$ and $KAl(SO_4)_2.12H_2O$ /22/ and of $(NH_3CH_3)Al(SO_4)_2.12H_2O$ /23,24/. Data for the quadrupol coupling constants and their temperature dependences are reported in /25-30/. In the recent years a large number of electron spin resonance studies has been published /31-36/. These studies supply important information about the position of the paramagnetic ion and in general on the temperature behaviour of the alums.

The connection between the crystal structure and thermal stability of the alums is discussed by Cudy /37/. The dynamical behaviour of the sulfate group within the alums was studied by diffraction methods by Ledsham, Steeple and Huges /38/. An extensive discussion of the crystallography of the alums is given by Haussühl /39/.

The crystal structure of alums has been studied first in the case of $KAl(SO_4)_2.12H_2O$ by Lipson and Beevers /40/. None of the alums has been investigated by modern counting techniques although Okaya, Ahmed, Pepinsky and Vand /41/ have studied $(NH_3CH_3)Al(SO_4)_2.12H_2O$ by photographic methods and refined the structure by least-squares calculations.

By now refinement of the crystal structure of a large number of alums has been studied from X-ray or neutron diffraction data and quite accurate results are available for:
$NaAl(SO_4)_2.12H_2O$ /42/, $CsAl(SO_4)_2.12H_2O$ /43/, K,Rb and $NH_4Al(SO_4)_2.12H_2O$ /44/ $ND_4Al(SO_4)_2.12D_2O$ /45/, $(NH_3CH_3)Al(SO_4)_2.12H_2O$ /46-50/, $NaCr(SO_4)_2.12H_2O$ /51/, $KCr(SO_4)_2.12H_2O$ /52/, $RbCr(SO_4)_2.12H_2O$ /53/, $(NH_3CH_3)Cr(SO_4)_2.12H_2O$ /54/ and $CsTi(SO_4)_2.12H_2O$ /55/.

1.1 Basic Information about the Alum Structure

Alum crystals can be grown quite easily as large single crystals with several mm to cm dimensions from saturated aqueous solutions. They have cubic symmetry at room temperature with the space group $Pa3\text{-}T_h^6$ although this symmetry can be achieved in case of ammonium and substituted ammonium alums only statistically. The unit cell contains 4 chemical units.

Early X-ray measurements by Lipson and Beevers /40/ and by Lipson /56/ were mainly made on aluminium sulfate alums. Their investigations showed that the alums crystallize polymorphous and that they can be classified as α, β and γ-alums according to their structure type. The type of alum formed depends upon the size of the monovalent cation. The α-structure, which represents the most common type, occurs if the cation is of intermediate size. The β-structure is observed with large cations, and the γ-structure with the smallest cations. A survey of a number of different alums and their structure types is given in Table 1. The listing is arranged according to the increasing size of the free monovalent ion.

Klug /58/ later investigated several alums where the trivalent ion was chromium. His results indicate that the chromium alums do not necessarily show the same classification scheme as their aluminium analogues. According to Klug the chromium alums of both rubidium and thallium belong to the β-structure whereas the corresponding aluminium alums have the α-class structure. Klug's deductions, however, are based on the evaluation of only a limited number of reflections. In a later investigation by Ledsham and Steeple /53/ rubidium chromium alum and thallium chromium alum are classified in the α-class structure. It can be seen from Table 1, that there is only with sodium as monovalent ion a difference between the structure of the aluminium and chromium alums. In methylammonium alums, too, the influence of the trivalent ion on the structure type is visible. The dimorphism

of the α and β-type appears more often in the chromium alum than in the aluminium alum. Thus, the structure type of a given alum is determined mainly by the size of the free monovalent ion, and generally the influence of the trivalent ion is not so strong as was first presumed by Ledsham and Steeple /47/

Table 1. Reference survey on alums

M^+	T^{3+}	Alum	Structure type	References
Na	Al	$(SO_4)_2.12H_2O$	γ	/42/ and /56/
K	Al	$(SO_4)_2.12H_2O$	α	/40/ and /44/
NH_4	Al	$(SO_4)_2.12H_2O$	α	/44/
ND_4	Al	$(SO_4)_2.12D_2O$	α	/45/
Rb	Al	$(SO_4)_2.12H_2O$	α	/44/
Tl	Al	$(SO_4)_2.12H_2O$	α	/42/
NH_3CH_3	Al	$(SO_4)_2.12H_2O$	α or β	/46-50/
Cs	Al	$(SO_4)_2.12H_2O$	β	/43/ and /56/
Na	Cr	$(SO_4)_2.12H_2O$	α	/51/
K	Cr	$(SO_4)_2.12H_2O$	α	/52/ and /57/
NH_4	Cr	$(SO_4)_2.12H_2O$	α	/58/
Rb	Cr	$(SO_4)_2.12H_2O$	α	/53/
Tl	Cr	$(SO_4)_2.12H_2O$	α	/53/ and /58/
NH_3CH_3	Cr	$(SO_4)_2.12H_2O$	α or β	/54/
Cs	Cr	$(SO_4)_2.12H_2O$	β	/51/
Cs	Ti	$(SO_4)_2.12H_2O$	β	/55/

In all alums there are two crystallographically different water molecules associated with the monovalent or the trivalent cations. The trivalent cation is surrounded by six water molecules with about

octahedral coordination but the orientation of the octahedron with respect to the cell axes is different in each of the three types. The monovalent cation in the α and γ-alum, too, is surrounded by six water molecules. In the γ-alum these water molecules form a nearly regular octahedron. In α-alum the octahedron is compressed along the threefold axis. The large cation in β-alum can accommodate 12 oxygen neighbours. To attain this large coordination number the water octahedron is compressed along the threefold axis and stretched normal to this axis until it is nearly planar.

In the γ-alum structure, [$NaAl(SO_4)_2.12H_2O$ is the only known representative of this type], six water molecules approach the small sodium cation much more closely than in the α-alum structure. This motion cannot take place unless the hydrogen bonding system changes. The most striking result is that the sulfate group becomes oppositely oriented along the threefold axis.

The reason for this may best be understood by looking at a monovalent ion M^+ of varying radius. Suppose it is such that the α-structure is formed. As the radius increases, each H_2O which touches the monovalent ion will move nearer to the other groups touching each other, and these will tend to alter their orientation to preserve correct distances. This change, however, is limited, and accompanied by a translation of the (RO_4) group along the threefold axis. This movement of the (RO_4) groups such as to decrease their distances from M^+, which also is increasing in size. When the attraction between the two is sufficient to become a governing factor in the structure, then the (RO_4) group takes up a new equilibrium position under the extra forces involved. The addition of bonds to M^+ will tend to change the disposition of the other bond, presumably the complete distribution will tend to be as uniform as possible.

If the radius of M^+ in the α-structure decreases, the associated water molecules will move further from the other groups. The resulting increase in the distance H_2O—O cannot be sufficiently corrected by translation of the (RO_4) groups along the threefold axis, since the oxygens in the α-structure are nearly at the minimum distance from M^+. If the (RO_4), however, is oppositely oriented along the threefold axis, the distance M^+—O can be much smaller, and thus a structure can be built up with a small distance M^+—H_2O. This is the structure of the γ-class.

1.2 Goal of this Work

In this work accurate X-ray and neutron diffraction measurements are reported on three aluminium sulfate dodecahydrate alums:

NH_4	Al $(SO_4)_2.12H_2O$	Ammonium-alum	(AASD)
(NH_3CH_3)	Al $(SO_4)_2.12H_2O$	Methylammonium-alum	(MASD)
(NH_3OH)	Al $(SO_4)_2.12H_2O$	Hydroxylammonium-alum	(HASD)

The structure determination is concentrated on three main problems:

1) The exact localization of the atoms of the ammonium group NH_4 and of the ammonium-substituted groups (NH_3CH_3) and (NH_3OH), specially of the hydrogen atoms.

When the centro-symmetric cubic space group $Pa3\text{-}T_h^6$ shall be sustained, atoms of these groups must be arranged statistically around 4(b) sites. Table 2 lists the atomic distribution of the atoms on the crystallographic sites in $Pa3\text{-}T_h^6$ /59/.

Table 2. Atomic positions for $^{\$}M$ Al $(SO_4)_2.12H_2O$-alums in $Pa3\text{-}T_h^6$

4 M	at(b): $\frac{1}{2}\frac{1}{2}\frac{1}{2}$, etc.	
4 Al	at(a): 000, etc.	
8 S	at(c): xxx, etc.	
8 $O_s(1)$	(one oxygen atom of the SO_4 group, on body diagonal) at(c): x´x´x´, etc.	
24 $O_s(2)$	oxygen atoms of SO_4 group other than $O_s(1)$ at(d): $x_1y_1z_1$, etc.	
24 $O_w(1)$	(oxygen atoms of water molecules coordinated to Al atoms) at(d): $x_2y_2z_2$, etc.	
24 $O_w(2)$	(oxygen atoms of water molecules coordinated to M groups) at(d): $x_3y_3z_3$, etc.	
24 H(1)	hydrogen atoms of $O_w(1)$	at(d): $x_4y_4z_4$, etc.
24 H(2)	hydrogen atoms of $O_w(1)$	at(d): $x_5y_5z_5$, etc.
24 H(3)	hydrogen atoms of $O_w(2)$	at(d): $x_6y_6z_6$, etc.
24 H(4)	hydrogen atoms of $O_w(2)$	at(d): $x_7y_7z_7$, etc.

$ M represents the NH_4, (NH_3CH_3) and (NH_3OH) groups.

2) The localization of the hydrogen atoms of the water molecules.

The accurate knowledge of the hydrogen positions is of importance for the understanding of the alum structure, where hydrogen bonding plays an essential role. Of special interest is the linearity of O-H····O links.

3) The behaviour of the SO_4 groups.

In the alum structure, the sulfate tetrahedra are arranged with the sulfur and one oxygen atom on the threefold axis and with three symmetry related oxygen atoms in a general position around this axis. For the oxygen atoms, and in particular for that on the threefold axis, abnormally high values for the temperature factors were found in former structure investigations. Bacon and Gardner /57/ explained this anomalous behaviour by a rotation of the oxygen atoms around the sulfur atom. The interpretation of Larson and Cromer /41/ was a structural disorder of the sulfate groups. Ledsham, Steeple and Hughes /38/ analysed the abnormal behaviour of the temperature factors of the oxygen atoms in the SO_4 groups by different oscillations of equal probability around three axes passing through the sulfur atom and through each of the three oxygen atoms in general position.

2. PRINCIPLES OF SINGLE CRYSTAL STRUCTURE ANALYSIS

2.1 Scattering Process

For neutron diffraction, the wave length λ of a neutron beam is described by the de Broglie relation

$$\lambda = \frac{h}{mv} = \frac{2\pi\hbar}{mv} = \frac{2\pi}{|\underline{k}|} \qquad 2.1$$

where m is the mass of the neutron, v its velocity and $\underline{k}$ the wave vector. The kinetic energies of thermal neutrons are in the range of 0.002 to 0.3 eV corresponding to λ = 6.39 to 0.52 A^{o} and are thus comparable with the energies of the thermal motion in the crystal. The energy of the X-ray quantum on the other hand is of the order of 10^{4} eV. In neutron diffraction experiments we observe a diffracted intensity which depends on the scattering vector defined by

$$\underline{S} = \underline{k}_o - \underline{k} \qquad 2.2$$

where

$\underline{k}_o$ and $\underline{k}$ are the wave vectors of the incident and the diffracted beams respectively, with

$$|\underline{k}_o| = \frac{2\pi}{\lambda} \qquad 2.3$$

For elastic scattering, the incident and diffracted beams have the same energy, therefore

$$|\underline{k}_o| = |\underline{k}| \qquad 2.4$$

and we have only to analyse the angular distribution of the intensity From Fig.1 we have

$$\sin\theta = \frac{|\underline{S}|}{2|\underline{k}_o|} \qquad 2.5$$

and with 2.3, we get

$$|\underline{S}| = \frac{4\pi}{\lambda} \sin\theta \qquad 2.6$$

If we define the interplanar spacing $d = \frac{2\pi}{|\underline{S}|}$ we have Bragg's law

$$\lambda = 2d.\sin\theta \qquad 2.7$$

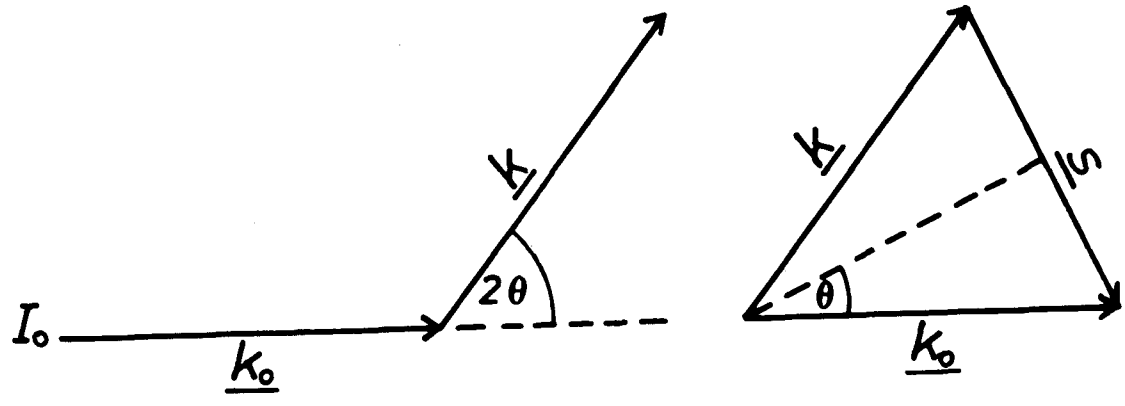

Fig.1: Relation between the incident and diffracted beam for elastic scattering described by Bragg's law.

If we treat the diffraction of X-ray or neutron through the interferences from the three dimensional lattice, we arrive at the Laue equations, which are /60/.

$$\underline{S} \cdot \underline{a}_1 = (\underline{s} - \underline{s}_o)\,\underline{a}_1 = h$$
$$\underline{S} \cdot \underline{a}_2 = (\underline{s} - \underline{s}_o)\,\underline{a}_2 = k$$
$$\underline{S} \cdot \underline{a}_3 = (\underline{s} - \underline{s}_o)\,\underline{a}_3 = l$$

where

$\underline{s}_o$ is the vector representing the incident wave,

$\underline{s}$ is the vector representing the reflected wave,

$\underline{S}$ is the scattering vector,

h,k and l are the Miller indices of the reflecting plane,

and $\underline{a}_1$, $\underline{a}_2$ and $\underline{a}_3$ are the basis vectors of the unit cell.

2.2. Four Circle Diffractometer

2.2.1 Definition of diffractometer angles (compare /61/)

The instrumental arrangement of a four circle diffractometer is illustrated in Fig.2, where the instrument axis is perpendicular to a horizontal plane passing through the centre of the instrument. The primary beam lies in this horizontal plane and is directed to the sample which is

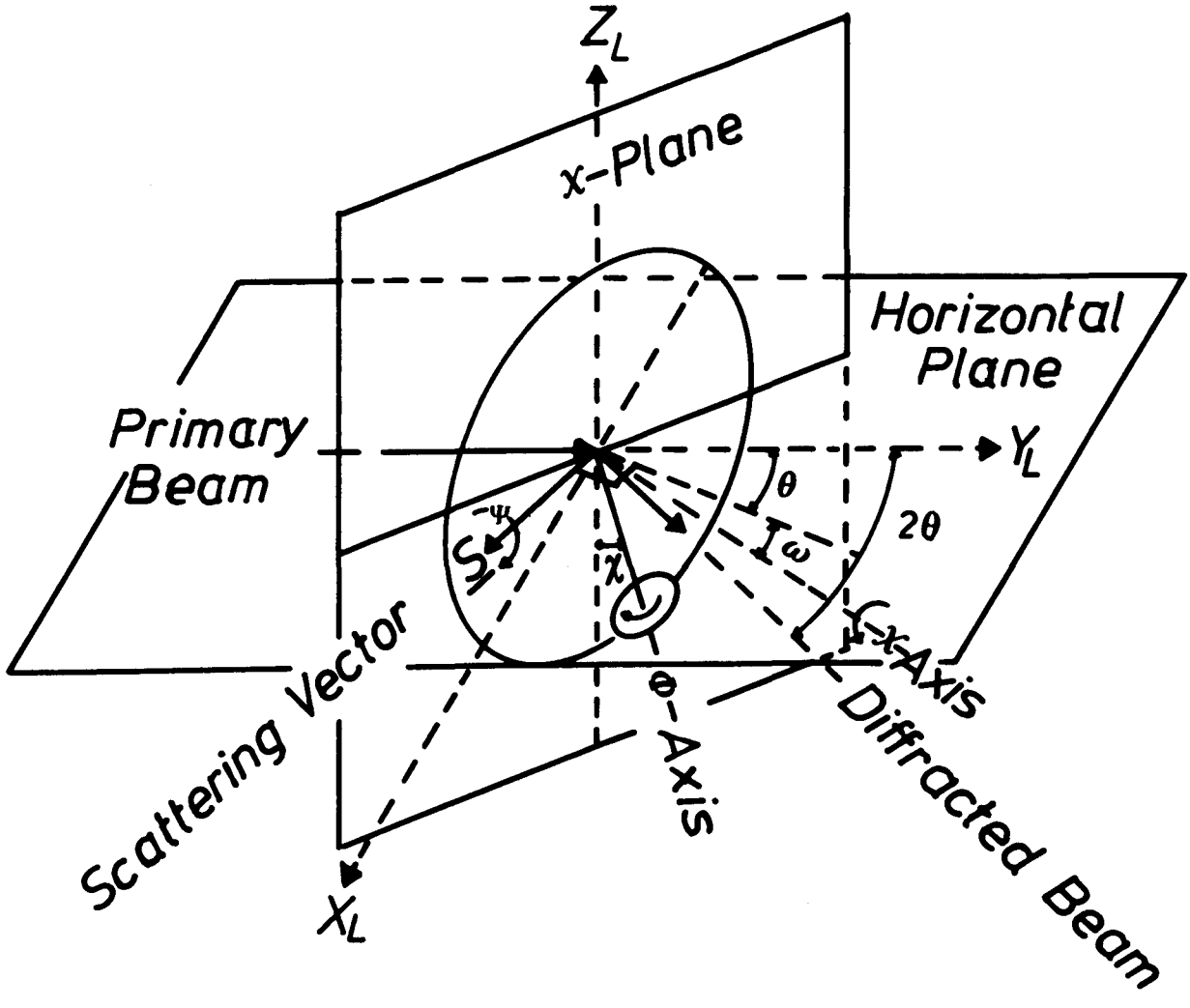

Fig.2: Schematic representation of a four circle diffractometer.

located at the instrument centre. The counter also lies in the horizontal plane and rotates around the instrument axis to make an angle 2θ with the primary beam direction. The instrument angles may be adjusted so that a

diffracted beam is horizontal and enters the centre of the counter.

Moving the counter through an angle of 2θ causes the crystal orienter and sample to turn through an angle of θ around the vertical axis. The orienter may also be rotated independently through an additional angle ω around the same axis. In this way the χ-axis which lies in the horizontal plane is positioned to make an angle of $\theta+\omega$ with the primary beam direction. The reflecting-plane normal (scattering vector), which bisects the angle between the diffracted beam and the reverse primary beam, thus makes an angle of ω with the plane of the χ-ring.

The Φ-shaft is supported from the χ-ring which permits the Φ-axis to be set at an angle χ from the vertical instrument axis. The sample is assumed to be rigidly attached to the Φ-shaft so that it can be turned around this axis.

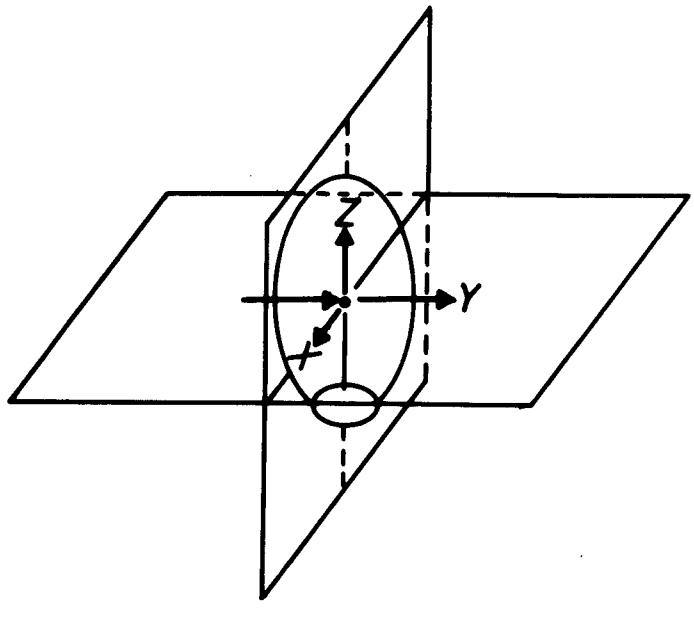

Fig.3: The four circle diffractometer with all angles set to zero.

The diffractometer with all angles set to zero is shown in Fig.3. The senses of θ , 2θ, ω and χ are defined by Fig.2, which shows the four circle diffractometer with these angles in the first quadrant.

The zero position for φ is chosen arbitrarily, and Fig.2 shows the direction of rotation which increases this angle.

The angle ψ shown in Fig.2 measures the rotation of the sample around the normal to the reflecting plane of interest. With this type of four circle diffractometer, ψ motion is achieved not by the rotation of a single shaft, but rather as a result of a combination of changes in ω , χ and φ .

2.2.2 Coordinate transformations

Let $\underline{h}_c$ be a vector in terms of the right-hand reciprocal lattice vectors $\underline{b}_1$, $\underline{b}_2$ and $\underline{b}_3$. According to the transformations from Patterson /62/ and Rollet /63/ this vector $\underline{h}_c$ can be described in terms of the crystal cartesian axes using the lattice matrix $\underline{B}$. If we choose the x_c-axis parallel to $\underline{b}_1$, the y_c-axis in the plane of $\underline{b}_1$ and $\underline{b}_2$, and the z_c-axis perpendicular to that plane as shown in Fig.4, then

$$\underline{h}_c = \underline{B} \cdot \underline{h} \qquad 2.8$$

where

$$\underline{B} = \begin{pmatrix} b_1 & b_2\cos\beta_3 & b_3\cos\beta_2 \\ 0 & b_2\sin\beta_3 & -b_3\sin\beta_2\cos\alpha_1 \\ 0 & 0 & 1/a_3 \end{pmatrix} \qquad 2.9$$

Here the a_j's and α_j's and b_j's and β_j's are the direct and the reciprocal parameters, respectively.

The orientation of the crystal with respect to the axes of the instrument is unknown at the start of the experiment.

The crystal is mounted on the goniometer head whose axis coincides with the Φ-axis of the instrument. Therefore we shall take another system of coordinates, the Φ-axis system, where the z-axis coincides with the Φ-axis.

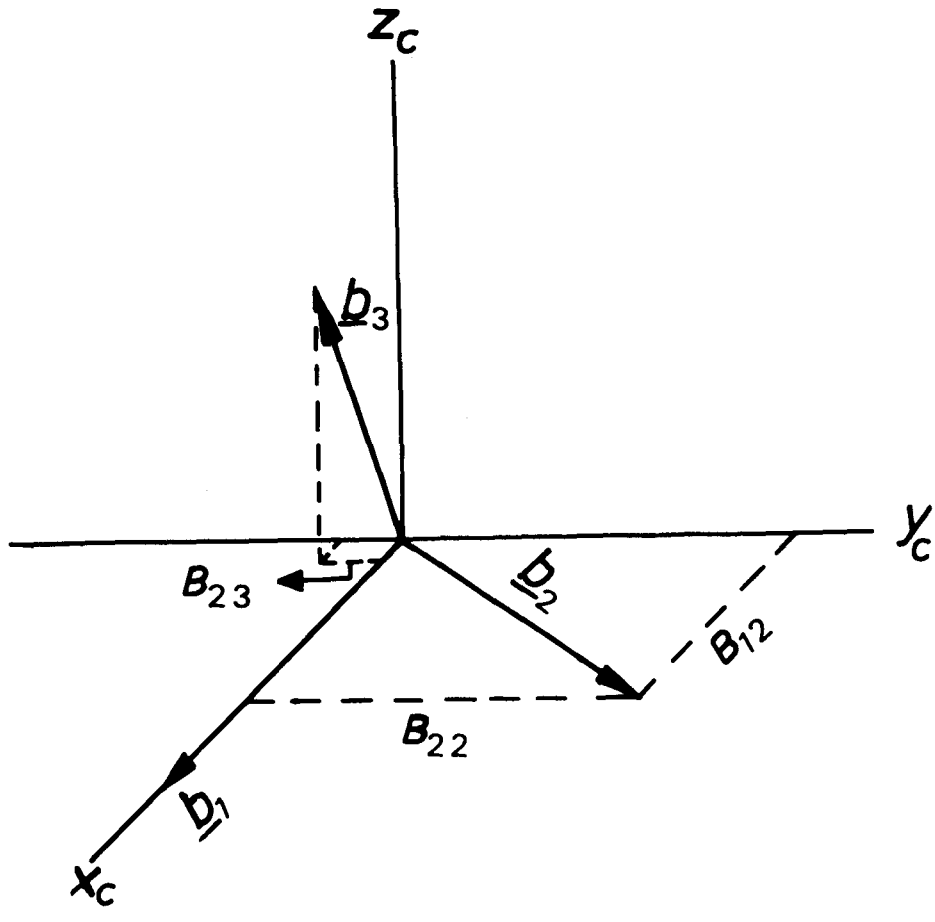

Fig.4: The relation between the reciprocal lattice vectors b_1, b_2, b_3, and the crystal cartesian axes x_c, y_c, z_c.

Let $\underline{U}$ be the orthogonal matrix which relates the Φ-axis system to the crystal cartesian system so that

$$\underline{h}_\varphi = \underline{U} \cdot \underline{h}_c \qquad 2.10$$

$\underline{U}$ will be called the orientation matrix since it depends on the way in which the crystal has been mounted, (since the crystal can be rotated about three angles in space φ, χ and ω as shown in Fig.5), and also on the arc settings

of the goniometer head.

In a similar way we can define three more cartesian systems attached to χ, Ω and Θ axes, respectively, and coincident with the Φ-axis system when all instrument angles are zero.

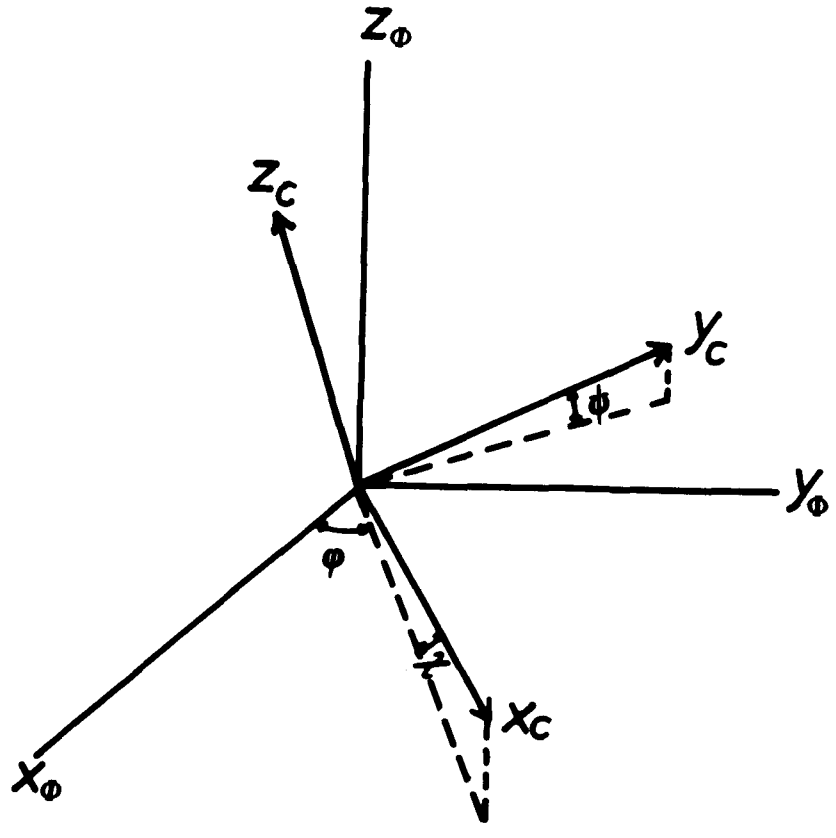

Fig.5: The rotation of the Φ-system with respect to the crystal cartesian coordinates.

Then we have the following relations:

$$\underline{h}_\chi = \underline{\Phi}\,\underline{h} \qquad 2.11$$

$$\underline{h}_\omega = \underline{\chi}\,\underline{h} \qquad 2.12$$

$$\underline{h}_\theta = \underline{\Omega}\,\underline{h} \qquad 2.13$$

where

$$\underline{\Phi} = \begin{pmatrix} \cos\varphi & \sin\varphi & 0 \\ -\sin\varphi & \cos\varphi & 0 \\ 0 & 0 & 1 \end{pmatrix} \qquad 2.14$$

(describing the rotation about the z-axis in the Φ-system)

$$\underline{\chi} = \begin{pmatrix} \cos\chi & 0 & \sin\chi \\ 0 & 1 & 0 \\ -\sin\chi & 0 & \cos\chi \end{pmatrix} \qquad 2.15$$

(describing the rotation about the y-axis in the χ-system)

$$\underline{\Omega} = \begin{pmatrix} \cos\omega & \sin\omega & 0 \\ -\sin\omega & \cos\omega & 0 \\ 0 & 0 & 1 \end{pmatrix} \qquad 2.16$$

(describing the rotation about the z-axis in the Ω-system)

Finally let us define a laboratory coordinate system X_1, Y_1 and Z_1 fixed with respect to the primary beam and a 2Θ-axis system attached to the counter shaft. Again these cartesian axes will be chosen to coincide with the Φ-axis system when all the instrument angles are zero, then we have

$$\underline{h}_1 = \underline{\theta} \cdot \underline{h} \qquad 2.17$$

where

$$\underline{\Theta} = \begin{pmatrix} \cos\theta & \sin\theta & 0 \\ -\sin\theta & \cos\theta & 0 \\ 0 & 0 & 1 \end{pmatrix} \qquad 2.18$$

with the rotation matrix

$$\underline{R} = \underline{\Omega}\,\underline{\chi}\,\underline{\Phi} \qquad 2.19$$

expanding equation 3.19 we have:

$$\underline{R} = \begin{pmatrix} \cos\omega\cos\chi\cos\varphi - \sin\omega\sin\varphi & \cos\omega\cos\chi\sin\varphi + \sin\omega\cos\varphi & \cos\omega\sin\chi \\ -\sin\omega\cos\chi\cos\varphi - \cos\omega\sin\varphi & -\sin\omega\cos\chi\sin\varphi + \cos\omega\cos\varphi & -\sin\omega\sin\chi \\ -\sin\chi\cos\varphi & -\sin\chi\sin\varphi & \cos\chi \end{pmatrix} \qquad 2.20$$

We will assume in the following discussion that we have an ideal diffractometer setting, i.e., a perfect diffractometer, a centered point sample with no mosaic spread, and a point source of monochromatic radiation. The deviations from these assumptions which are found in practice usually do not invalidate the calculations to be described.

To observe a reflection in the ideal diffractometer setting, it is necessary for θ to satisfy the Bragg equation and the scattering vector $\underline{S}$ to be perpendicular to the χ-axis, this means that the scattering vector lies along the positive χ-axis of the Θ-coordinate system and we have for $\underline{S}$:

$$\underline{S} = \begin{pmatrix} 1 \\ 0 \\ 0 \end{pmatrix} d^* \qquad 2.21$$

where d^* is the reciprocal of the interplanar spacing in Angstrom units and is given for example by the equation

$$d^*_{\underline{h}} = \sqrt{(h_{c1})^2 + (h_{c2})^2 + (h_{c3})^2} \qquad 2.22$$

where

$$h_c = \underline{B} \cdot \underline{h} \qquad 2.23$$

$$\sin\theta = \lambda \cdot d^*/2 \qquad 2.24$$

From equation 2.20, we can write

$$\underline{S} = \underline{R}\,\underline{U}\,\underline{B}\,\underline{h} \qquad 2.25$$

From equations 2.21 and 2.25, we have

$$\underline{R}^{-1} \begin{pmatrix} 1 \\ 0 \\ 0 \end{pmatrix} d^* = \underline{U}\,\underline{B}\,\underline{h} = \underline{h} \qquad 2.26$$

Expanding equation 2.26, we have

$$\begin{pmatrix} \cos\omega\cos\chi\cos\varphi - \sin\omega\sin\varphi \\ \cos\omega\cos\chi\sin\varphi + \sin\omega\cos\varphi \\ \cos\omega\sin\chi \end{pmatrix} d^* = \underline{U}\,\underline{B}\,\underline{h} \qquad 2.27$$

With a four circle diffractometer the reflecting condition can be established in an unlimited number of ways corresponding to various values of ψ , the angle of rotation of the sample around the scattering vector.

2.2.3 Calculation of the U-matrix from three reflections

When the unit cell parameters are unknown it is still possible to obtain the matrix UB if the setting angles can be observed for at least three independent reflections with known (or assumed) indices. Given $2\theta_i$, ω_i, χ_i and φ_i for reflection i, we can compute the scattering

vector in the Φ-axis system:

$$\underline{h}_{\varphi i} = \frac{2\sin\theta_i}{\lambda} \begin{pmatrix} \cos\omega_i \cos\chi_i \cos\varphi_i - \sin\omega_i \sin\varphi_i \\ \cos\omega_i \cos\chi_i \sin\varphi_i + \sin\omega_i \cos\varphi_i \\ \cos\omega_i \sin\chi_i \end{pmatrix} \qquad 2.28$$

For each of the three reflections the matrix $\underline{UB}$ must perform the following transformation

$$\underline{h}_{\varphi i} = \underline{U}\,\underline{B}\,\underline{h}_i \qquad 2.29$$

where $\underline{h}_i$ is the vector of indices. If $\underline{H}_\varphi$ is a matrix made up of the three column vectors $\underline{h}_{\varphi i}$, and $\underline{H}$ is constructed analogous from $\underline{h}_i$, we have

$$\underline{H}_\varphi = \underline{U}\,\underline{B}\,\underline{H} = \begin{pmatrix} h_{x\varphi 1} & h_{x\varphi 2} & h_{x\varphi 3} \\ h_{y\varphi 1} & h_{y\varphi 2} & h_{y\varphi 3} \\ h_{z\varphi 1} & h_{z\varphi 2} & h_{z\varphi 3} \end{pmatrix} = \underline{U}.\underline{B} \begin{pmatrix} h_1 & h_2 & h_3 \\ k_1 & k_2 & k_2 \\ l_1 & l_2 & l_3 \end{pmatrix} \qquad 2.30$$

The reflections chosen must correspond to the reciprocal lattice vectors which are not coplanar or the matrix $\underline{H}$ will be singular. The indices should be assigned so that the vectors can be described with reference to a right-handed coordinate system, and it can be shown that the determinant $|\underline{UB}|$ will be positive if and only if this condition is fulfilled.

Having obtained the matrix $\underline{UB}$ it is possible to derive the corresponding cell parameters. Let us compute the matrix

$$(\underline{U}.\underline{B})'(\underline{U}.\underline{B}) = \underline{B}'\underline{U}'\underline{U}\,\underline{B} \qquad 2.31$$

and since $\underline{U}$ is orthogonal, then $\underline{U}' = \underline{U}^{-1}$ and from equation 2.31 we have

$$(\underline{U}.\underline{B})\ (\underline{U}.\underline{B})' = \underline{B}'\ \underline{B} \qquad 2.32$$

or

$$(\underline{B}'\ \underline{B})^{-1} = \underline{G} \qquad 2.33$$

where $\underline{G}$ is a matrix (see for example Patterson /59/) in the form

$$\underline{G} = \begin{pmatrix} a_1^2 & a_1a_2\cos\alpha_3 & a_1a_3\cos\alpha_2 \\ a_1a_2\cos\alpha_3 & a_2^2 & a_2a_3\cos\alpha_1 \\ a_1a_3\cos\alpha_2 & a_2a_3\cos\alpha_1 & a_3^2 \end{pmatrix} \qquad 2.34$$

By substitution of the lattice parameters in equation 2.29, we can determine the $\underline{B}$ matrix. Then we can calculate the $\underline{U}$-matrix using the relation

$$\underline{U} = (\underline{U}\ \underline{B})\ \underline{B}^{-1} \qquad 2.35$$

2.3. Data Handling

2.3.1 Structure factor and temperature factor

The unit cell of a crystal contains atoms in various positions with various scattering powers. The diffracted wave is described by a structure factor given by the expression

$$F_{hkl} = \sum_j f_j \, e^{2\pi i(hx_j + ky_j + lz_j)} \, e^{-B_j(\sin\theta/\lambda)^2} \qquad \text{for X-rays} \qquad 2.36$$

$$F_{hkl} = \sum_j b_j \, e^{2\pi i(hx_j + ky_j + lz_j)} \, e^{-B_j(\sin\theta/\lambda)^2} \qquad \text{for neutrons} \qquad 2.37$$

In the case of X-rays f_j is the scattering factor of the $j^{\underline{th}}$ atom depending on $\sin\theta/\lambda$. In the case of neutrons b_j is the scattering length. In the case of the nuclear scattering there is no dependence of b_j on $\sin\theta/\lambda$.

B_j is related to the mean-square amplitude of the atomic vibration.

In general the vibrations of the atoms are anisotropic. Then the temperature factor expression for each atom considered is

$$\exp\Big[-1/4(B_{11}h^2a^{*2} + B_{22}k^2b^{*2} + B_{33}l^2c^{*2} + 2B_{12}hk.a^*b^*\cos\gamma^* + 2B_{13}hl.a^*c^*\cos\beta^* + 2B_{23}kl.b^*c^*\cos\alpha^*)\Big] \qquad 2.38\text{-a}$$

or

$$\exp\Big[-(\beta_{11}h^2 + \beta_{22}k^2 + \beta_{33}l^2 + 2\beta_{12}hk + 2\beta_{13}hl + 2\beta_{23}kl)\Big] \qquad 2.38\text{-b}$$

where B_{ij} and β_{ij} are the components of a symmetric tensor describing an ellipsoid surface.

2.3.2 Intensity data reduction

The observed intensity I_{hkl} is related to the structure factor amplitude $|F_{hkl}|$ by

$$I_{hkl} = I_o.K.L.P.A.E.|F_{hkl}|^2 \qquad 2.39$$

$$= K'.L.P.A.E.|F_{hkl}|^2$$

where I_o is the intensity of the incident beam,

K' is the scale factor,

L is the Lorentz factor,

P is the polarization factor (in case of X-ray only),

A is the absorption correction ($\approx$ transmission)

and E is the extinction correction.

The scaling K' is a constant for a given data set depending on the experimental setting, including for example the collimator and detector efficiency, on the crystal volume and on the wave length. It is not known at the beginning.

The Lorentz factor L depends on the measurement technique used. For single crystal X-ray and neutron diffraction, the Lorentz correction is given by

$$L = \frac{1}{\sin 2\theta} \qquad 2.40$$

The polarization factor P is restricted to X-ray scattering and is given by (including a monochromator crystal with take-off angle T)

$$P = \frac{1 + \cos^2 T.\cos^2 2\theta}{2(1 + \cos^2 T)} + \frac{1 + \cos T.\cos 2\theta}{2(1 + \cos T)} \qquad 2.41$$

The absorption correction A depends upon the path length of the beam through the crystal and on the magnitude of the absorption coefficient μ of the compound. The transmission factor is given by

$$A_{hkl} = \frac{1}{V} \int \exp - \left[\mu(p+q)\right] dv \qquad 2.42$$

p and q are the path lengths of the incident and the reflected beam in the crystal and V is the volume of the crystal.

The crystals studied here were spheres and in this case the integration A_{hkl} over all path lengths is tabulated for given values of μR and θ , where R is the radius of the crystal /64-66/.

The extinction E considers the intensity attenuation of a diffracted beam due to two different physical processes known as primary and secondary extinction. Primary extinction results from an interference process from subsequent reflections yielding finally for a perfect crystal a diffracted intensity to be proportional to $|F|$ rather than $|F^2|$. Secondary extinction influences reflections of high intensities where an amount of the incident beam is reflected by the first planes. The deeper planes thus receive less incident intensity and thus the scattered intensity of these planes is reduced. The secondary extinction for a mosaic crystal of arbitrary shape was estimated by Zachariasen /67/ by the expression

$$F_{corr.} = F_{obs} \left[1 + g \left(\frac{1 + \cos^4 2\theta}{1 + \cos^2 2\theta} \right) F_{obs} / \sin 2\theta \right]^{-1/4} \qquad 2.43$$

where g is the secondary extinction coefficient. For all the structure refinements in this work, the expression 2.43 has been used.

2.3.3 Calculation of the structure factor

The usual procedure in a crystal structure analysis is to determine experimentally the values $|F_{hkl}^{obs}|$ from the measured integrated intensities I_{hkl} (see equ. 2.39) for as many planes as possible. Knowing the sorts and the number of atoms or ions in the unit cell, all the peculiarities of intensity distribution are next used in order to decide the most probable values of x,y,z for each atom or ion. The approximate values of x,y,z so obtained, when substituted in equations 2.36 or 2.37, should give values of F_{hkl}^{calc}, not too far from the observed values $|F_{hkl}^{obs}|$ for all observed reflections. In other words, the values of the quantity $R = \sum(|F_{obs}| - |F_{calc}|) / \sum|F_{obs}|$ should be small (0.25 to 0.15). At this step we may assume to have a correct model for the crystal structure.

2.3.4 Fourier technique

As a next step for the calculation of improved structure factors for a given electron or nuclear distribution, one performs the inverse operation, i.e., one calculates the electron or the nuclear density distribution, $\rho_{(x,y,z)}$, by a given set of structure factors. Since a crystal possesses periodicity, the unit cell content can be described by Fourier series. For the three-dimensional case, the Fourier representation is given by the expression

$$\rho_{(x,y,z)} = \frac{1}{V} \sum_h \sum_k \sum_l F_{hkl}\, e^{-2\pi i(hx + ky + lz)} \qquad 2.44$$

where h,k,l are integers between $-\infty$ and ∞ and V is the unit cell volume.

An alternative expression for a three-dimensional Fourier series can be obtained by noting that the structure factor can be written

in the form

$$F_{hkl} = \left|F_{hkl}\right| e^{2\pi i \alpha'_{hkl}} = \left|F_{hkl}\right| e^{i\alpha_{hkl}}$$

where $2\pi\alpha'_{hkl}$ is the phase angle. Substituting this in equ. 2.44, we can write

$$\rho_{(x,y,z)} = \frac{1}{V} \sum_h \sum_k \sum_l \left|F^{obs}_{hkl}\right| e^{-2\pi i(hx + ky + lz)} e^{i\alpha^{calc}_{hkl}} \qquad 2.45$$

The values of $\left|F^{obs}_{hkl}\right|$ are taken from the experiment, but due to equation 2.45, for the purpose of Fourier analysis the value of the phase angle α_{hkl} (or the sign + or -) must be known. This quantity α_{hkl} is lost during the diffraction experiment and cannot directly be determined from the scattering experiment (which yields F^2-values). This phase angle α^{calc}_{hkl} is calculated from the structural model as follows:

$$\left|F^{calc}_{hkl}\right| = \sqrt{A^2_{hkl} + B^2_{hkl}} \qquad 2.46$$

with $$A^{calc}_{hkl} = \sum_j f_j \cos 2\pi (hx_j + ky_j + lz_j) \qquad 2.47$$

and $$B^{calc}_{hkl} = \sum_j f_j \sin 2\pi (hx_j + ky_j + lz_j) \qquad 2.48$$

The phase angle α_{hkl} is then given by the expression

$$\alpha^{calc}_{hkl} = \tan^{-1} \frac{B^{calc}_{hkl}}{A^{calc}_{hkl}} \qquad 2.49$$

When the differences between the observed structure amplitudes and the calculated structure amplitudes with the phase α^{calc}_{hkl} are used as coefficients in a Fourier analysis $\left(\left|F^{obs}_{hkl}\right| - \left|F^{calc}_{hkl}\right|\right)$, then we have a difference Fourier synthesis. From this, the difference between the observed density distribution (described by F^{obs}_{hkl}) and the density distribution due to the structure model (described by F^{calc}_{hkl}) should be seen. Based on this difference distribution, additional atoms can be localized

or better positions assigned than before, and then new structure factors, with improved phases, can be calculated. This process can be repeated several times until a satisfactory fit is reached. Equations 2.47 and 2.48 are for the case of X-rays. For neutron diffraction we replace f_j by b_j.

2.3.5 Least-squares refinement

Once the model derived by difference Fourier analysis is correct, the best obtainable parameters can be calculated by least-squares methods. The least-squares method in crystal structure refinement is based on a mathematical comparison of a given structure model described by model structure factors F_{calc} with the observed values $|F_{obs}|$. By varying the parameters of the function F_{calc}, the expression

$$\sum_{hkl} \left(|F_{obs}| - |K.F_{calc}| \right)^2 \qquad 2.50$$

is minimized.

The agreement between the observations and calculations is commonly expressed by residual factors, like R or R_w, where

$$R = \frac{\sum_{hkl} \left| |F_{obs}| - |K.F_{calc}| \right|^2}{\sum_{hkl} |F_{obs}|^2} \qquad 2.51$$

and

$$R_w = \frac{\sum_{hkl} w_{hkl} \left| |F_{obs}| - |K.F_{calc}| \right|^2}{\sum_{hkl} w_{hkl} |F_{obs}|^2} \qquad 2.52$$

w_{hkl} are the weights given to the observations, for example according to an expression given by Cruickshank /68/

$$w_{hkl} = A|F_{obs}|^2 + B|F_{obs}| + C \qquad 2.53$$

3. EXPERIMENTAL

3.1 Crystal Growth

Large single crystals of alums had been grown from aqueous solution by cooling /29/, since alums show in general a fairly large positive coefficient of solubility in water. The crystals used in this work were kindly provided by Prof. Weiss, Darmstadt and Prof. Recker, Bonn. Single crystals of ammonium and methylammonium aluminium sulfate dodecahydrate were grown by slow cooling of saturated aqueous solution. The rate in cooling $\Delta T/\Delta t$ was $0.05^{\circ}C$/hour and $0.03^{\circ}C$/hour in the range of temperature $T_{max} = 40^{\circ}C$, $T_{min} = 25^{\circ}C$ and $T_{max} = 45^{\circ}C$, $T_{min} = 20^{\circ}C$ in the case of ammonium and methylammonium alums respectively. In the case of hydroxylammonium alum, the crystals were grown by evaporating water from the saturated solution at constant temperature of $22^{\circ}C$. A careful thermostatisation of the solution was applied in all growth experiments to avoid unwanted formation of nuclei and to gain undistorted single crystals.

3.2 X-ray Diffractometer

The X-ray diffraction data were collected on an automatic four-circle diffractometer SYNTEX $P2_1$ of Bonn University. The wave length used was Mo-K_α radiation ($\lambda = 0.7107$ Å) in connection with a graphite monochromator ($2\Theta_m = T = 12.2^{\circ}$). The unit cell parameters in the case of ammonium and methylammonium alums were determined by least-squares calculations from the adjusted angular settings of 25 independent reflections. The intensity measurements were carried out in the Θ-2Θ scan mode with a 1.0° plus (α_1,α_2)-dispersion scan range. The scan speed was adjustable between 0.5 and 10.0° per minute, and the total background counting time equalled the time spent for the peak counting. Six standard reflections, 10 0 0, $\overline{10}$ 0 0, 0 10 0, 0 $\overline{10}$ 0

0 0 10 and 0 0 $\overline{10}$, were remeasured after every 28 reflections.

3.3 Neutron Diffractometer

Neutron diffraction data were collected on the Bonn University computer controlled neutron four circle diffractometer NANCY /69/ at the DIDO research reactor, Kernforschungsanlage Jülich. The wave length used was λ = 1.2868 Å taken from a Cu(111)-monochromator. Again the orientation matrix and the lattice constants of each crystal were determined by least-squares analysis from the optimized angular positions of 12 independent reflections. The peak intensity measurements were carried out by step scanning in the Θ-2Θ scan mode at intervals of $\Delta(2\Theta) = 0.1^{\circ}$ and at a rate of 2.2 degree/30 minutes. The standard reflection 3 3 3 was remeasured after every 9 reflections. The measured scan data were processed semi-automatically on a PDP8 computer via Tektronix video screen by calculating first a spline function through the data points, which was then used to calculate the integrated intensities and the background /70/.

4. RESULTS OF $NH_4Al(SO_4)_2.12H_2O$ ALUM

4.1. X-Ray Measurements

4.1.1 Experimental data

The X-ray diffraction data were collected from a single crystal of ammonium aluminium sulfate dodecahydrate alum, $NH_4Al(SO_4)_2.12H_2O$ (AASD), of spherical shape with a diameter of 0.24 mm. Up to a maximum angle $2\Theta = 90^\circ$ a total number of 4813 reflections was recorded.

In the data reduction, the intensities were adjusted to the fluctuation of the sum of the standard reflections. Symmetry related reflections were averaged resulting in a set of 905 unique reflections, of which 419 were regarded as unobserved $\left[I<2.0\sigma(I)\right]$. The internal agreement index of the data based on the deviation of the $|F_{h,i}|$ of equivalent reflections from their means $|\bar{F}_h|$ was:

$$R_f = \sum_h \sum_i \left| |\bar{F}_h| - |F_{h,i}| \right| \Big/ \sum_h \sum_i |F_{h,i}| = 0.027$$

The experimental data are summarized in Table 3.

Table 3. Crystallographic and experimental data for X-ray diffraction

Crystal diameter (mm)	0.24
Maximum Θ-angle ($^\circ$)	45
$(\sin\Theta/\lambda)_{max}$ ($\AA^{-1}$)	0.995
Scan mode	Θ-2Θ
Number of steps/scan	96
Number of monitor reflections	6
Monitor reflections interval	28
Lattice constant ($\AA$)	12.242(1)
Number of reflections recorded	4813
Number of unique reflections	905
Number of unobserved reflections	419
μ (cm^{-1}), μR	4.36, 0.052
Transmission for $2\Theta = 0^\circ$ and $2\Theta = 60^\circ$	92.79%, 92.81%

With an absorption coefficient of $\mu = 4.36\ cm^{-1}$ and a sphere of 0.024 cm diameter, the transmission is 92,79% for $2\Theta = 0^{\circ}$ and 92,81% for $2\Theta = 60^{\circ}$. Correction for absorption can be neglected therefore.

4.1.2 Structure refinement

From the structure refinement of $KAl(SO_4)_2.12H_2O$ /40/, the atomic positions of the skeleton $Al(SO_4)_2.12H_2O$, neglecting the hydrogen atoms of the water molecules, were taken as starting values for the structure analysis. Scattering factors for neutral atoms as given in the International Tables for X-ray Crystallography /71/ were used.

From three-dimensional difference Fourier maps a positive peak was observed at the centre of symmetry, $\frac{1}{2}\ \frac{1}{2}\ \frac{1}{2}$, which was attributed to the nitrogen atom of the ammonium group. A full-matrix least-squares refinement at this stage with isotropic temperature factors was computed after adding the position of the nitrogen atom. After several cycles the residual R factor was 0.13. When the structure at this stage did not refine further, the nitrogen atom obviously experiences positional disorder and must be removed from the centre of symmetry at 4(b) $\frac{1}{2}\ \frac{1}{2}\ \frac{1}{2}$ into the position 8(c) xxx. This means a statistical distribution of the nitrogen atoms over two crystallographic sites. With this model refinement could be carried on to R = 0.11.

An essential improvement was achieved by including the information about the localization of the hydrogen atoms and of disordered SO_4 groups due to the neutron data analysis (4.2.2). The final positional and thermal parameters are given in Tables 6a and 6b (lower numbers). A comparison of observed structure amplitudes and calculated structure factors is given in Table /74/.

4.2 Neutron Measurements

4.2.1 Experimental data

For the neutron diffraction measurements a single crystal was ground to a sphere of 3.8 mm diameter. Up to $2\Theta_{max} = 65^{\circ}$ a total of 3360 reflections in the six octants hkl, $\bar{h}\bar{k}\bar{l}$, $hk\bar{l}$, $\bar{h}\bar{k}l$, $h\bar{k}\bar{l}$ and $\bar{h}kl$ was measured. Due to the cubic symmetry relation of the space group Pa3, hkl = lhk = klh, each reflection has been measured 18 times. Symmetry related reflections were averaged resulting in a set of 190 unique reflections, of which 50 reflection were considered unobserved according to $\left[I < 2.0\sigma(I) \right]$ The absorption coefficient was determined experimentally to $\mu = 2.46\ cm^{-1}$ and correction of absorption was considered negligible ($\mu R = 0.47$, transmission = 50.28% for $2\Theta = 0^{\circ}$ and 51.20% for $2\Theta = 60^{\circ}$, i.e., the difference in absorption is less than 1%). The crystallographic and experimental data are given in Table 4.

Table 4. Crystallographic and experimental data for neutron diffraction

Crystal diameter (mm)	3.8
Maximum 2Θ-angle ($^{\circ}$)	65
Scan mode	Θ-2Θ
Number of steps/scan	23
Number of monitor reflections	1
Monitor reflections interval	9
Lattice constant (Å)	12.248
Number of reflections recorded	3360
Number of unique reflections	190
Number of unobserved reflections	50
μ (cm^{-1}), μR	2.46, 0.47
Transmission for $2\Theta = 0^{\circ}$ and $2\Theta = 60^{\circ}$	50.28%, 51.20%

4.2.2 Structure refinement

The positions of the heavy atoms were taken from the X-ray refinement as starting values for the structure analysis but without the nitrogen atom. From a three-dimensional difference Fourier map the positions of the hydrogen atoms of the water molecules and all the atoms of the $(NH_4)^+$ group could be identified immediately (Fig.6). Two peaks on the threefold body diagonal were recognized, one positive representing N and one negative (because of the negative scattering length of hydrogen) representing one of the four hydrogen atoms of the $(NH_4)^+$ group. The other three hydrogen atoms of the $(NH_4)^+$ group occupy a general position at 24(d).

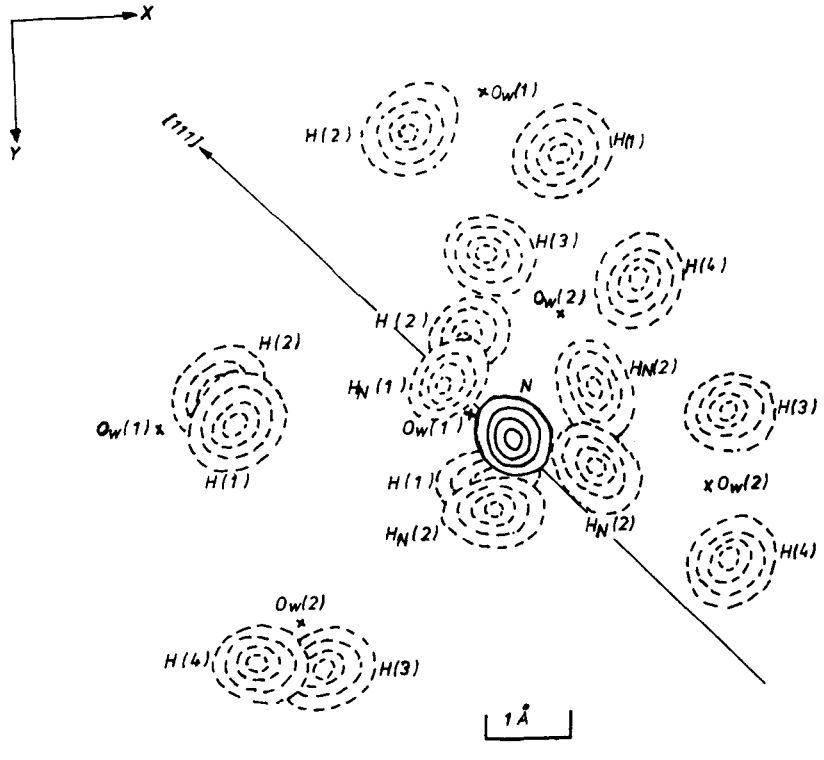

Fig.6. Difference Fourier map around $\frac{1}{2}\ \frac{1}{2}\ \frac{1}{2}$ with $z \leqq 0.5$.

Additionally the hydrogen atoms of the water molecules are visible as negative maxima in the difference Fourier map. Fig.6 depicts a section of

this difference Fourier map around $\frac{1}{2}\ \frac{1}{2}\ \frac{1}{2}$ with $z \leqq 0.5$. It is clear from this map that the $(NH_4)^+$ group is disordered on two positions related to each other by inversion through the centre of symmetry. In this way an improved structure model could be deduced with the approximate hydrogen positions of the water molecules and of the ammonium group and with the nitrogen atom lying at xxx in 8(c) with $x = 0.5 \pm 0.01$. A full-matrix least-squares refinement based on this model and regarding isotropic thermal parameters for all atoms resulted in R = 0.093. Admitting anisotropic temperature factors for all atoms, using the weighting scheme given by equation 2.53 and an isotropic extinction correction given by equation 2.43, the R factor reduced from 0.093 to 0.058.

The thermal parameters for the sulfate oxygen atoms were found to be unusually large in comparison to the normal behaviour of the other thermal parameters. To overcome this, a further difference Fourier map was calculated yielding two relatively small positive peaks (Fig.7): One peak being on the threefold axis on the opposite side of the sulfur atom from $O_S(1)$ and the other in a general position. These Fourier maxima form a tetrahedral environment around the sulfur atom, consequently some of the sulfate groups are in a reversed orientation around the sulfur atom.

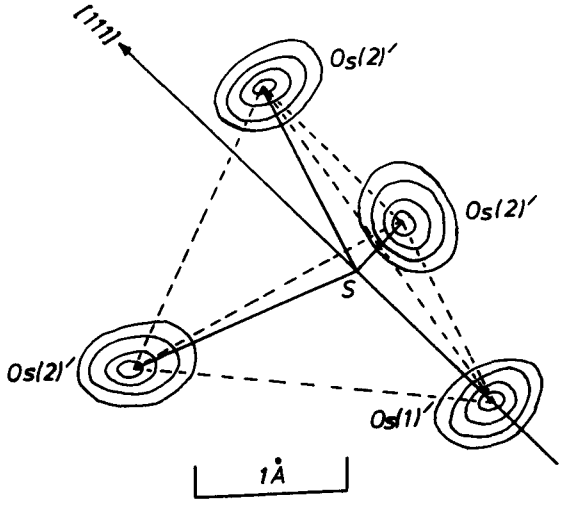

Fig.7. Difference Fourier map arround S shows the disordered tetrahedron.

A least-squares refinement was then calculated including a disorder parameter k (percentage of the disorder) in the list of variables. The fraction of the reversed sulfate oxygen atoms $O_s(1)'$ and $O_s(2)'$ was set equal to k, the fraction of the sulfate oxygen atoms $O_s(1)$ and $O_s(2)$, in the normal positions to (1-k). With this model the refinement was continued with anisotropic temperature factors for all atoms and including the weighting scheme (2.53) and the correction for isotropic extinction (2.43) resulting in $R_w = 0.014$. Comparison of the thermal parameters and the values of the R factors without and with disorder parameter of the sulfate oxygen for the neutron data are given in Table 5.

Table 5. Comparison of thermal parameters and R factors for ordered and disordered (SO_4) groups from neutron data

		ordered (SO_4) k = 0%	disordered (SO_4) k = 16.9%
$O_s(1)$	B_{11}	7.6	5.7
	B_{12}	0.6	0.1
	B_{equ}	7.6	5.7
$O_s(2)$	B_{11}	3.4	2.7
	B_{22}	6.9	5.0
	B_{33}	4.7	3.2
	B_{12}	2.5	1.8
	B_{13}	1.8	1.2
	B_{23}	3.6	2.2
	B_{equ}	5.0	3.6

$$B_{ij} = 4.a^2 \beta_{ij} \quad , B_{equ} = 4/3\ a^2(B_{11} + B_{22} + B_{33})$$

	Agreement values	
R	0.064	0.044
$R_{o.u.}$	0.046	0.025
R_w	0.028	0.015
$R_{w.o.u.}$	0.026	0.014

o.u. omitting unobserved

The final atomic positions and temperature factors due to the structure refinement of the neutron data are summerized in Tables 6a and 6b respectively (upper numbers).

Table 6a. Fractional atomic coordinates ($x10^4$) with e.s.d's in parentheses for neutron (upper numbers) and X-ray (lower numbers).

Atom	Wyckoff position	Site	Occupancy	x	y	z
Al	4(a)	000	1.0			
S	8(c)	xxx	1.0	3111(11) 3083(1)		
$O_s(1)$	8(c)	xxx	0.831	2385(9) 2401(5)		
$O_s(1)'$	8(c)	xxx	0.169	3831(39) 3709(33)		
$O_s(2)$	24(d)	xyz	0.831	3137(2) 3130(2)	2640(3) 2652(2)	4199(2) 4199(2)
$O_s(2)'$	24(d)	xyz	0.169	2105(13) 2098(8)	3556(28) 3701(11)	2823(16) 2889(8)
N	8(c)	xxx	0.5	5070(8) 5082(11)		
$H_N(1)$	8(c)	xxx	0.5	4389(44)		
$H_N(2)$	24(d)	xyz	0.5	4375(7)	4969(18)	5314(7)
$O_w(1)$	24(d)	xyz	1.0	177(2) 171(1)	-171(2) -162(1)	1530(2) 1520(1)
$O_w(2)$	24(d)	xyz	1.0	442(2) 454(1)	1367(2) 1377(1)	2990(2) 2979(1)
H(1)	24(d)	xyz	1.0	275(3)	432(3)	2059(3)
H(2)	24(d)	xyz	1.0	429(3)	9171(3)	1874(3)
H(3)	24(d)	xyz	1.0	-42(4)	1965(3)	2834(4)
H(4)	24(d)	xyz	1.0	1182(4)	1676(3)	2937(4)

Table 6b. Atomic thermal parameters β_{ij} ($\times 10^4$) with e.s.d's in parentheses for neutron (upper numbers) and X-ray (lower numbers). B_{equ} is included for comparison with previous investigations.

Atom	β_{11}	β_{22}	β_{33}	β_{12}	β_{13}	β_{23}	B_{equ}
Al	32(9) 27(1)			0 0			1.9 1.7
S	67(12) 34(1)			12(17) 6(1)			4.0 2.0
$O_s(1)$	95(8) 78(4)			1(13) -21(5)			5.7 4.7
$O_s(1)'$	161(70) 149(10)			-77(67) -62(8)			9.7 8.9
$O_s(2)$	45(3) 55(1)	83(3) 84(2)	52(3) 45(1)	29(4) 30(2)	20(2) 12(2)	36(3) 33(1)	3.6 3.7
$O_s(2)'$	58(21) 100(9)	367(52) 218(17)	142(27) 103(9)	72(28) 142(10)	-21(17) 53(7)	90(32) 134(10)	11.3 8.4
N	27(4) 48(5)			-13(6) 3(7)			1.6 2.9
$H_N(1)$	179(64)			95(77)			10.7
$H_N(2)$	116(9)	251(16)	37(10)	-10(14)	28(5)	-54(14)	8.1
$O_w(1)$	57(3) 47(1)	22(3) 38(1)	40(3) 27(1)	-10(3) 1(1)	5(2) -3(1)	-11(2) 1(1)	2.4 2.2
$O_w(2)$	63(4) 59(1)	34(3) 47(1)	62(3) 55(1)	-5(3) 5(1)	19(2) -11(1)	-7(3) -9(7)	3.2 3.2
H(1)	56(5)	87(6)	42(5)	-1(4)	-1(3)	6(4)	4.9
H(2)	85(5)	42(4)	37(3)	7(4)	-35(4)	6(3)	3.3
H(3)	90(6)	89(6)	64(5)	12(4)	-21(5)	-5(4)	4.9
H(4)	92(6)	86(5)	132(6)	4(5)	-59(5)	-40(5)	6.2

The final values for the weighting scheme w, the secondary extinction coefficient g, the residual R factors and the goodnes of the fit are given in Table 7 together with the analogous X-ray data. A comparison between the observed structure amplitudes and the calculated structure factors for neutron diffraction is given in Table /74/.

Table 7. Values of w, g, R factors and goodnes of the fit for X-ray and neutron data in AASD alum.

	X-ray	neutron
a) w [according to (2.53)]	$2.5 \quad \lvert F\rvert \geqq 50$	$0.35 \quad \lvert F\rvert \geqq 150$
	$0.0008\lvert F\rvert^2 + 0.01\lvert F\rvert + 0.002 \quad \lvert F\rvert < 50$	$0.000015\lvert F\rvert^2 + 0.0001\lvert F\rvert + 0.002 \quad \lvert F\rvert < 150$
b) g [according to (2.43)]	$2.6(1)\times10^{-6}$	$12.1(7)\times10^{-6}$
c) Agreement values		
R (all reflections)	0.053	0.044
R (observed reflections)	0.033	0.025
R_w (all reflections)	0.024	0.015
R_w (observed reflections)	0.024	0.014
d) Goodnes of fit	0.922	0.885

4.3 Discussion of the Structure

The structure of the AASD, $NH_4Al(SO_4)_2.12H_2O$, alum is characteristic of the α-alum type. The character of the compound is ionic with positive Al^{3+} ions and $(NH_4)^+$ groups and negative $(SO_4)^{2-}$ groups. There are 12 water molecules on two crystallographically different sites, six surrounding the aluminium ion and the other six the ammonium group. Table 8 lists important interatomic distances and angles. In the following, the details of the different groups are discussed.

i) Six water molecules $O_w(1)$ with H(1) and H(2) surround each aluminium ion in the form of a regular octahedron as shown in Fig.8. The Al-$O_w(1)$ distance is 1.897(2)Å. The distances $O_w(1)$-$O_w(1)$ are 2.693(1) and 2.671(5)Å with a mean distance for the edges of this octahedron of 2.682 ± 0.011 . Within the water molecules we find $O_w(1)$-H distances of 0.989(9) and 0.960(4)Å for H(1) and H(2) respectively and an angle H(1)-$O_w(1)$-H (2) of 107.4(4)°.

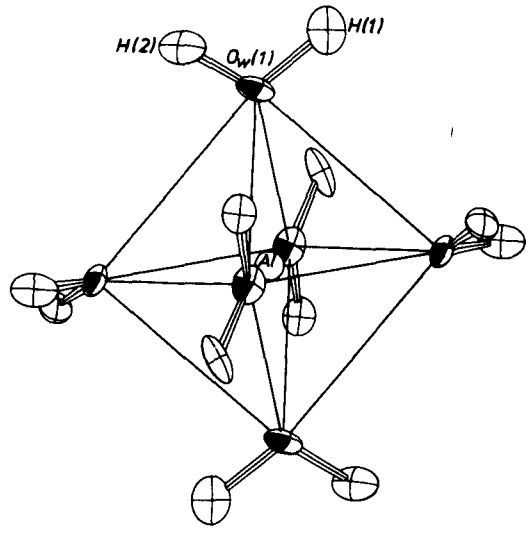

Fig.8. The regular octahedron of the six water molecules surrounding the Al^{3+} ion

Table 8. Interatomic distances (Å) and angles (°) with e.s.d's in parentheses from neutron data in AASD alum.

distances in (Å)		angles in (°)	
1) Al-6O$_w$(1) octahedron			
Al-O$_w$(1)	1.897(2)		
O$_w$(1)-O$_w$(1)	2.693(1)	O$_w$(1)-Al-O$_w$(1)	90.5(1)
O$_w$(1)-O$_w$(1)	2.671(5)	O$_w$(1)-Al-O$_w$(1)	89.5(1)
<O$_w$(1)-O$_w$(1)>	2.682		
2) $(NH_4)^+$ group			
N-O$_w$(2)	2.990(3)	O$_w$(2)-N-O$_w$(2)	115.8(2)
N-O$_w$(2′)	3.065(5)	O$_w$(2′)-N-O$_w$(2′)	111.5(3)
N-H$_N$(1)	1.15(11)	H$_N$(1)-N-H$_N$(2)	115.3(4)
N-H$_N$(2)	0.91(1)	H$_N$(2)-N-H$_N$(2)	103.1(4)
<N-O$_w$(2)>	3.028	<O$_w$(2)-N-O$_w$(2)>	113.7
<N-H$_N$>	1.03	<H$_N$-N-H$_N$>	109.2
3) Order $(SO_4)^{2-}$ group			
S-O$_s$(1)	1.539(5)	O$_s$(1)-S-O$_s$(2)	108.2(7)
S-O$_s$(2)	1.452(7)	O$_s$(2)-S-O$_s$(2)	110.7(7)
O$_s$(1)-O$_s$(2)	2.423(12)	O$_s$(2)-O$_s$(1)-O$_s$(2)	59.1(2)
O$_s$(2)-O$_s$(2)	2.388(1)	O$_s$(2)-O$_s$(2)-O$_s$(1)	60.5(2)
		O$_s$(2)-O$_s$(2)-O$_s$(2)	60.0
<S-O$_s$>	1.496	<O$_s$-S-O$_s$>	109.5
<O$_s$-O$_s$>	2.406	<O$_s$-O$_s$-O$_s$>	59.9

Table 8. (Continued)

	distances in (Å)		angles in (°)
4) Disorder $(SO_4)^{2-}$ group			
S-$O_s(1)'$	1.52(6)	$O_s(1)'$-S-$O_s(2)'$	115.5(8)
S-$O_s(2)'$	1.39(1)	$O_s(2)'$-S-$O_s(2)'$	102.8(10)
$O_s(1)'$-$O_s(2)'$	2.47(4)	$O_s(2)'$-$O_s(1)'$-$O_s(2)'$	52.3(4)
$O_s(2)'$-$O_s(2)'$	2.18(2)	$O_s(2)'$-$O_s(2)'$-$O_s(1)'$	63.9(1)
		$O_s(2)'$-$O_s(2)'$-$O_s(2)'$	60.0
$<S-O_s'>$	1.46	$<O_s'-S-O_s'>$	109.2
$<O_s'-O_s'>$	2.33	$<O_s'-O_s'-O_s'>$	58.7
5) Water molecules			
$O_w(1)$-H(1)	0.989(9)		
$O_w(1)$-H(2)	0.960(4)	H(1)-$O_w(1)$-H(2)	107.4(4)
H(1)-H(2)	1.571(1)		
$<O_w(1)-H>$	0.975		
$O_w(2)$-H(3)	0.953(1)		
$O_w(2)$-H(4)	0.984(2)	H(3)-$O_w(2)$-H(4)	105.6(5)
H(3)-H(4)	1.543(7)		
$<O_w(2)-H>$	0.969		
$<O_w-H>$	0.972		
<H-H>	1.557	$<H-O_w-H>$	106.5

ii) The $(NH_4)^+$ group is coordinated by the other six water molecules in the form of a highly distorted octahedron as shown in Fig.9 (for simplicity, the reversed $(NH_4)^+$ group generated by inversion at $\frac{1}{2}\ \frac{1}{2}\ \frac{1}{2}$ has been omitted). Here we find $O_w(2)$-H = 0.984(2) and 0.953(1)Å for H(3) and H(4) respectively and an angle H(3)-$O_w(2)$-H(4) of 105.6(5)°. The nearest $O_w(2)$-$O_w(2)$ distances are 3.303(7)Å. These six water molecules can be separated into two groups $H_2O_w(2)$ and $H_2O_w(2')$ of three each. The distances between nitrogen and oxygen are N-$O_w(2)$ = 2.990(3)Å and N-$O_w(2')$ = 3.065(5)Å.

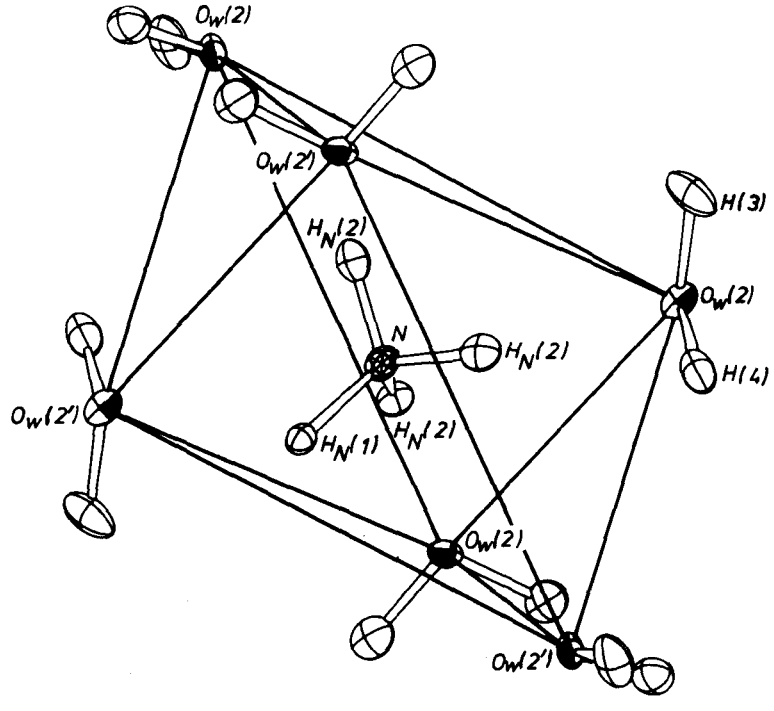

Fig.9. The distorted octahedron of the six water molecules surrounding the $(NH_4)^+$ group (only one orientation of the group is shown).

The $(NH_4)^+$ group itself shows a statistical distribution on two positions with equal probability. Fig.10a depicts the idealized configuration and Fig.10b shows the two orientations together. The distances in the $(NH_4)^+$ group are: N-$H_N(1)$ = 1.15(11)Å and N-$H_N(2)$ = 0.91(1)Å with

angles $H_N(1)$-N-$H_N(2)$ = 115.3(4)° and $H_N(2)$-N-$H_N(2)$ = 103.1(4)°. The mean <N-H_N> distances are 1.03Å with a mean angle < H_N-N-H_N > of 109.2°.

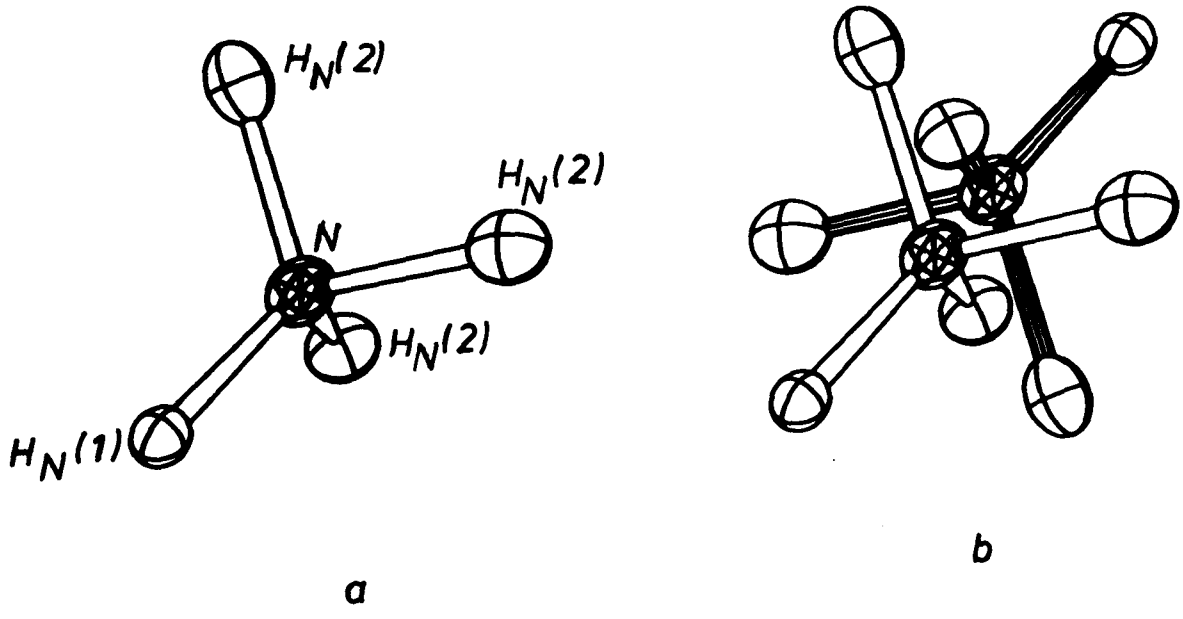

Fig.10. The $(NH_4)^+$ group.

a) Only one orientation.

b) The two orientations

Some of the $(SO_4)^{2-}$ groups are disordered, this means that the $(SO_4)^{2-}$ group can take two orientations around the sulfur atom in such a way that a certain percentage (k x 100) of the sulfate oxygens is in reversed orientation along the threefold axis. For describing this disorder we have introduced a disorder parameter k = 0.169(11). The two orientations are shown in Fig.11.

The normal sulfate oxygen atoms $O_s(1)$ and $O_s(2)$ form with the sulfur atom a regular tetrahedron with one oxygen $O_s(1)$ and the S atom on the threefold axis, and the remaining oxygen atoms $O_s(2)$ in general positions. The distances of this tetrahedron are: S-$O_s(1)$ = 1.539(5)Å

and S-$O_s(2)$ = 1.452(7)Å and the mean $< O_s\text{-}O_s >$ distance is 2.406Å with a mean angle $< O_s\text{-}S\text{-}O_s >$ of 109.5°.

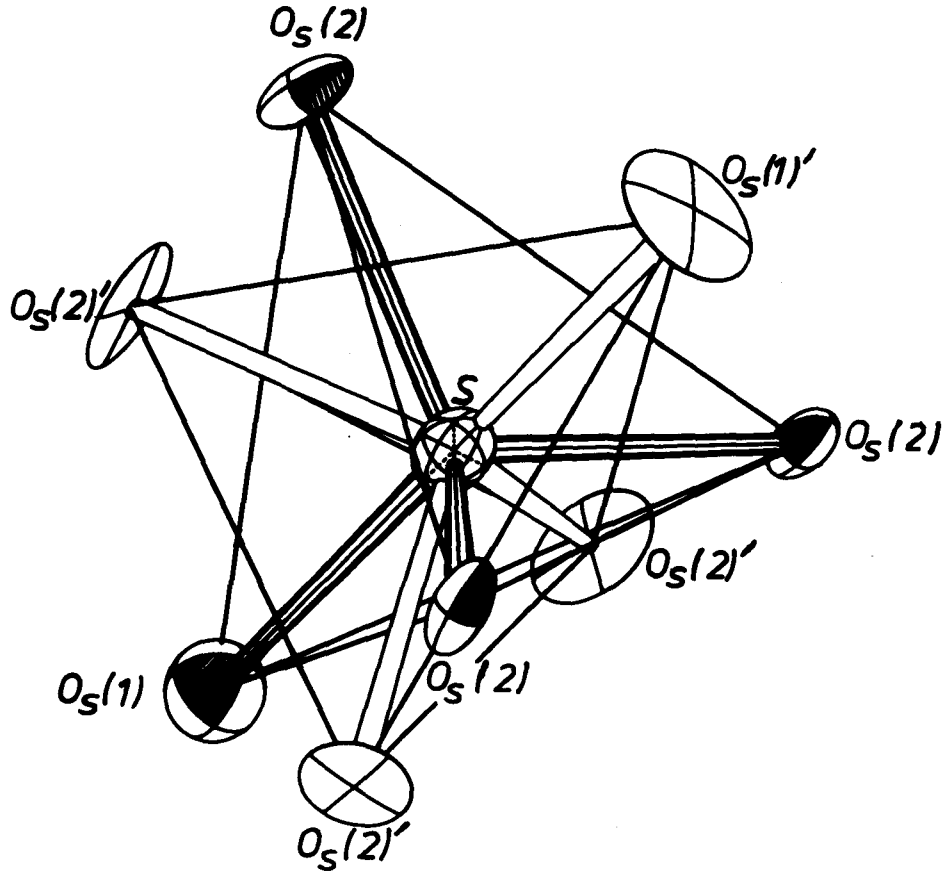

Fig.11. The two orientations of the $(SO_4)^{2-}$ group.

The reversed oxygen atoms $O_s(1)'$ and $O_s(2)'$ on the other hand form with the sulfur atom a distorted tetrahedron with S-O (1)' = 1.52(6)Å and S-$O_s(2)'$ = 1.39(1)Å. The mean $< O_s'\text{-}O_s' >$ distance is 2.33Å and the mean $< O'\text{-}S\text{-}O' >$ angle is 109.2°.

The hydrogen bond systems will be discussed later (Chapter 9) together with the analogous results of the other two alums.

5. RESULTS OF $(NH_3CH_3)Al(SO_4)_2.12H_2O$ ALUM

5.1. X-Ray Measurements

5.1.1 Experimental data

The X-ray diffraction data were collected from a single crystal of methylammonium aluminium sulfate dodecahydrate (MASD) alum, $(NH_3CH_3)Al(SO_4)_2.12H_2O$, of spherical shape with a diameter of 0.14 mm. The refined cubic unit cell parameter a = 12.322(3)Å is in reasanable agreement with 12.242(1)Å reported by Kozhin and Zaitseva /50/. Up to a maximum $2\Theta = 60^\circ$ the total number of measured reflections was 2196. Symmetry related reflections were averaged in a set of 877 unique reflections, of which 385 were regarded as unobserved according to the criterion $\left[I < 2.5\sigma(I)\right]$.

With an absorption coefficient of $\mu = 4.27\ cm^{-1}$ and an assumed sphere of 0.2 mm diameter, the transmission is 94.19% for $2\Theta = 0^\circ$ and 94.20% for $2\Theta = 60^\circ$. Correction for absorption can be neglected therefore.

5.1.2 Structure refinement

The crystal structure of MASD alum at room temperature has been analysed from X-ray diffraction by Lipson /46/ and by Fletcher and Steeple /48/. In these papers the atoms of the methylammonium group are considered as an entity to be located on the centre of symmetry at 4(b) $\frac{1}{2}\ \frac{1}{2}\ \frac{1}{2}$. Okaya et al. /41/ found that the methylammonium groups are statistically arranged and located in general position 24(d) xyz.

The atomic positions of the skeleton $Al(SO_4)_2.12H_2O$

of the AASD alum, neglecting the hydrogen atoms of the water molecules and the disorder in the (SO_4) tetrahedra (compare Table 6a) were used as starting values in a full-matrix least-squares refinement. From a three-dimensional difference Fourier map three positive peaks could be observed, one at the centre of symmetry $\frac{1}{2}\ \frac{1}{2}\ \frac{1}{2}$, the other two on the threefold body diagonal at xxx with x = $\pm$ 0.45. These three peaks were attributed to the nitrogen and the carbon atoms of the $(NH_3CH_3)^+$ group. The interpretation of further difference Fourier maps, in order to distinguish between the locations of the nitrogen and the carbon atoms in the first difference Fourier map, turned out to be ambiguous because nitrogen and carbon are nearly indistinguishable in X-ray diffraction analysis with atomic numbers 7 and 6 respectively.

This problem has been overcome by the refinement of the structure using neutron diffraction (see 5.2.2). This analysis revealed that the nitrogen lies at $\frac{1}{2}\ \frac{1}{2}\ \frac{1}{2}$ and the carbon on the threefold axis at $\pm$ xxx. More over the accurate positions of the hydrogen atoms of the water molecules and those of the $(NH_3CH_3)^+$ group could be determined only by the neutron data. Including the neutron diffraction information into the least-squares calculation, the X-ray refinement was continued with fixed hydrogen positions to an R factor of 0.10.

The decisive step for further improvement was to move the nitrogen atom from the centre of symmetry at 4(b) $\frac{1}{2}\ \frac{1}{2}\ \frac{1}{2}$ to the more general position 8(c) xxx on the threefold body diagonal like in AASD alum. Anisotropic temperature factors were then used for all non hydrogen atoms with weighting scheme (2.53) and an isotropic extinction correction (2.43). The final value of R_w was 0.030. The final values of the atomic and thermal parameters are given in Table 9a and 9b respectively (lower numbers). Observed structure amplitudes and calculated structure factors are tabulated in Table /74/.

5.2. Neutron Measurements

5.2.1 Experimental data

For the neutron diffraction measurements a single crystal of MASD alum was ground to a sphere of 3.2 mm diameter. Up to $2\Theta_{max} = 65^{o}$ a total number of 2288 reflections in the four octants hkl, $\bar{h}$kl, h$\bar{k}$l and hk$\bar{l}$ was measured resulting in a set of 194 unique reflections. Due to the criterion $\left[I < 2.5\sigma(I)\right]$, 42 reflections were considered unobserved.

The absorption was measured on a large flat single crystal yielding an absorption coefficient of $\mu = 2.06\ cm^{-1}$. With $\mu R = 0.33$ the transmission was 61.47% for $2\Theta = 0^{o}$ and 61,98% for $2\Theta = 60^{o}$. Correction for absorption can be neglected therefore.

5.2.2 Structure refinement

For the first calculation with the neutron diffraction data, the positional parameters of the heavy atoms from the X-ray results were taken as starting values without the position of the nitrogen atom. The position of the hydrogen atoms of the water molecules were taken from AASD alum as given in Table 6a. From three-dimensional difference Fourier maps, the locations of all the atoms of the $(NH_3CH_3)^+$ group could be identified immediately. Three positive peaks on the threefold body diagonal were recognized, representing N and C, and further 12 negative peaks representing the hydrogen atoms of the $(NH_3CH_3)^+$ group. The positive peaks representing N and C are slightly elongated along the threefold axis. One peak lies at the centre of symmetry $\frac{1}{2}\ \frac{1}{2}\ \frac{1}{2}$, and the other two positive peaks on the threefold body diagonal at xxx with $x = \pm 0.45$.

To differentiate between nitrogen (b_N = 9.40f) and carbon (b_c = 6.64f) a second three-dimensional difference Fourier map was calculated with b = 6.64f for both positions. The result was a strong positive peak at $\frac{1}{2}\ \frac{1}{2}\ \frac{1}{2}$ due to the positive difference of b_N-b_C. With b = 9.40f for both positions, two strong negative peaks were observed on the threefold body diagonal at xxx with x = $\pm$ 0.45 due to the negative values of the difference b_C-b_N.

From the above steps, it is clear that the nitrogen atom lies on the centre of symmetry $\frac{1}{2}\ \frac{1}{2}\ \frac{1}{2}$ and the carbon atom at xxx on the threefold axis. This means that the carbon atom occupies the position 8(c) with x = 0.45 which requires a statistical distribution over two positions each.

The hydrogens H(N) of the methylammonium group are located in the general positions 24(d) xyz with x = 0.58, y = 0.54 and z = 0.47 and the hydrogens H(C) also in 24(d) xyz with x = 0.38, y = 0.51 and z = 0.42. Thus the hydrogen atoms of the methylammonium group experience a statistical distribution over two sites around the nitrogen and the carbon atoms. Fig 12 depicts a section of the first difference Fourier map arround $\frac{1}{2}\ \frac{1}{2}\ \frac{1}{2}$ with z$\leqq$ 0.5, yielding two positive and six negative peaks, the other peaks are found in the map with z$\leqq$ 0.5.

With these informations, the structure refinement was carried on. Least-squares analysis with isotropic temperature factors was computed including all atoms leading to a residual R factor of 0.10. The refinement was continued by admitting the nitrogen atom to be statistically distributed around the centre of symmetry on the threefold axis at 8(c) rather than at 4(b), the R factor was reduced to 0.09.

Final refinement was carried out with anisotropic temperature factors for all atoms and including an isotropic secondary extinction coefficient (2.43) in the list of variables. At the last stage of refinement a weighting scheme (2.53) was supplied for all observations leading to R_w = 0.029.

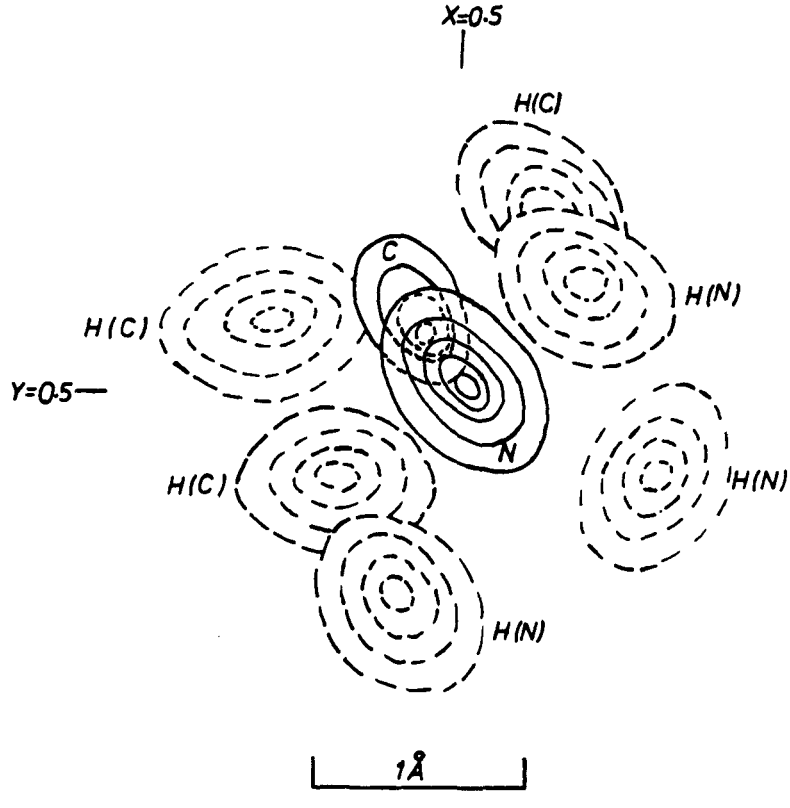

Fig.12. Difference Fourier map around $\frac{1}{2}\ \frac{1}{2}\ \frac{1}{2}$ with $z \leqq 0.5$.

The final atomic and thermal parameters taken from the last stage of refinement are given in Tables 9a and 9b respectively (upper numbers). The observed structure amplitudes and the calculated structure factors from parameters of Tables 9a and 9b are given in Table /74/.

Table 9a. Fractional atomic coordinates ($x10^4$) with e.s.d's in parentheses for neutron (upper numbers) and for X-ray (lower numbers).

Atom	Wyckoff position	Site	Occupancy	x	y	z
Al	4(a)	000	1			
S	8(c)	xxx	1	3022(15) 3020(2)		
$O_S(1)$	8(c)	xxx	1	2341(10) 2324(5)		
$O_S(2)$	24(d)	xyz	1	6911(3) 6932(2)	7530(5) 7523(2)	914(4) 917(2)
N	8(c)	xxx	1/2	5156(11) 5137(16)		
H(N)	24(d)	xyz	1/2	837(11)	5363(17)	275(19)
C	8(c)	xxx	1/2	4501(42) 4504(12)		
H(C)	24(d)	xyz	1/2	3851(52)	5072(56)	4134(53)
$O_W(1)$	24(d)	xyz	1	8521(3) 8497(1)	9810(3) 9803(1)	185(4) 197(1)
$O_W(2)$	24(d)	xyz	1	419(4) 420(1)	1373(4) 1351(1)	2975(3) 2965(1)
H(1)	24(d)	xyz	1	5423(4)	2018(5)	4728(5)
H(2)	24(d)	xyz	1	4132(6)	1846(5)	4502(6)
H(3)	24(d)	xyz	1	2143(5)	4941(6)	1944(6)
H(4)	24(d)	xyz	1	2148(5)	6103(6)	1697(5)

Table 9b. Atomic thermal parameters β_{ij} ($\times 10^4$) with e.s.d's in parentheses for neutron (upper numbers) and X-ray (lower numbers). B_{equ} is included for comparison with previous investigations.

Atom	β_{11}	β_{22}	β_{33}	β_{12}	β_{13}	β_{23}	B_{equ}
Al	30(1)			0			1.8
	37(2)			0			2.3
S	31(16)			-15(20)			1.9
	46(4)			12(2)			2.8
$O_s(1)$	80(11)			6(14)			4.9
	108(5)			-8(5)			6.6
$O_s(2)$	57(5)	118(5)	48(5)	-14(5)	17(4)	-51(4)	4.5
	65(1)	132(2)	75(2)	-42(2)	18(2)	-65(2)	5.5
N	44(13)			9(16)			2.7
	56(14)			-4(15)			3.4
H(N)	12(13)	120(23)	175(24)	10(13)	16(14)	17(19)	6.2
C	162(31)			-15(37)			9.8
	109(8)			-40(10)			6.6
H(C)	437(74)	499(72)	422(68)	-202(80)	49(45)	56(68)	27.5
$O_w(1)$	22(5)	44(5)	42(5)	-3(4)	11(4)	2(4)	2.2
	36(1)	51(1)	43(1)	-2(1)	4(1)	7(1)	2.6
$O_w(2)$	53(6)	56(5)	35(4)	-2(5)	-19(3)	-17(4)	2.9
	64(2)	57(2)	57(2)	-1(1)	-7(1)	-4(1)	3.6
H(1)	14(7)	44(7)	63(7)	-18(5)	-9(6)	-1(6)	2.5
H(2)	52(7)	41(6)	59(6)	21(6)	-19(6)	-5(6)	3.1
H(3)	66(9)	74(8)	63(9)	-8(7)	29(6)	23(7)	4.1
H(4)	90(9)	45(8)	63(7)	-5(6)	13(6)	1(7)	4.0

The final values of the weighting scheme w, the secondary extinction coefficient g, the R factors and the goodnes of the fit are given in Table 10 for X-ray and neutron data.

Table 10. Values of w, g, R factors and goodnes of the fit for X-ray and neutron data in MASD alum.

	X-ray	neutron
a) w [according to (2.53)]	$0.21 \quad \lvert F\rvert \geqq 180$	$0.41 \quad \lvert F\rvert \geqq 80$
	$0.000005\lvert F\rvert^2 + 0.0024\lvert F\rvert + 0.001 \quad \lvert F\rvert < 180$	$0.00004\lvert F\rvert^2 + 0.0019\lvert F\rvert + 0.001 \quad \lvert F\rvert < 80$
b) g [according to (2.43)]	$0.8(1)\times10^{-6}$	$98.1(7)\times10^{-6}$
c) Agreement values		
R (all reflections)	0.068	0.064
R (observed reflections)	0.043	0.051
R_w (all reflections)	0.031	0.030
R_w (observed reflections)	0.030	0.029
d) Goodnes of fit	1.058	0.880

5.3 Discussion of the Structure

Analogous to AASD alum, the aluminium ion is surrounded by six water molecules forming a nearly regular octahedron with Al-$O_w(1)$ distances of 1.851(5)Å and a mean $<O_w(1)-O_w(1)>$ distance of 2.618Å . Within the water molecules we find $O_w(1)$-H distances of 1.007(2)Å for H(1) and 1.029(12)Å for H(2) and an angle $\sphericalangle$H(1)-$O_w(1)$-H(2) of 106.4(5)°.

The other six water molecules are surrounding the $(NH_3CH_3)^+$ group in the form of a distorted octahedron as shown in Fig.13a. These six water molecules can be separated into two groups $H_2O_w(2)$ and $H_2O_w(2')$ of three each as shown in Fig.13b and 13c respectively. The distances between nitrogen and oxygen are N-$O_w(2)$ = 2.994(1)Å and N-$O_w(2')$ = 3.159(1)Å. The corresponding carbon-oxygen distances are 3.481(45) and 2.979(7)Å respectively. For this second group of water molecules the $O_w(2)$-H distances are shorter than in water molecules surrounding the aluminium ion, namelv $O_w(2)$-H(3) = 0.929(2)Å and $O_w(2)$-H(4) = 0.945(3)A and an angle $\sphericalangle$H(3)-$O_w(2)$-H(4) = 102.8(5)°.

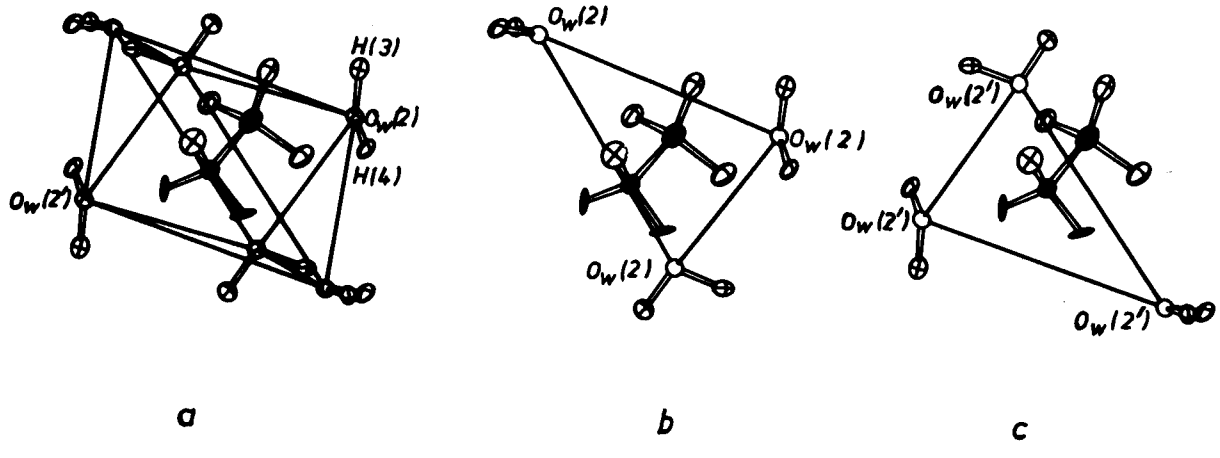

Fig.13. The $(NH_3CH_3)^+$ group with the surrounding six water molecules. (Only one orientation of the group is shown).

a) The distorted octahedron.
b) The $(NH_3CH_3)^+$ group with only three water molecules.
c) The $(NH_3CH_3)^+$ group with the [illegible]

The $(NH_3CH_3)^+$ group itself shows a statistical distribution on and around the threefold axis. Nitrogen and carbon, both occupy two positions on the threefold axis at 8(c). The shift from the centre of symmetry is $\pm$ 0.0166(11)Å for nitrogen and $\pm$ 0.0499(42)Å for carbon. The hydrogen atoms H(N) and H(C) are consequently also distributed around the threefold axis over two sites each in the general positions 24(d). This means in fact that the $(NH_3CH_3)^+$ group has two orientations related to each other by a centre of symmetry (Fig.14a). In Fig.14b the $(NH_3CH_3)^+$ group occupies one orientation in one unit cell and the other orientation (Fig.14c) in a second unit cell. The distances within one $(NH_3CH_3)^+$ group are 1.397(84)Å for C-N bond with bonding angles $\sphericalangle$H(N)-N-H(N) = 110.4(3)° and $\sphericalangle$H(C)-C-H(C) = 112.7(11)°.

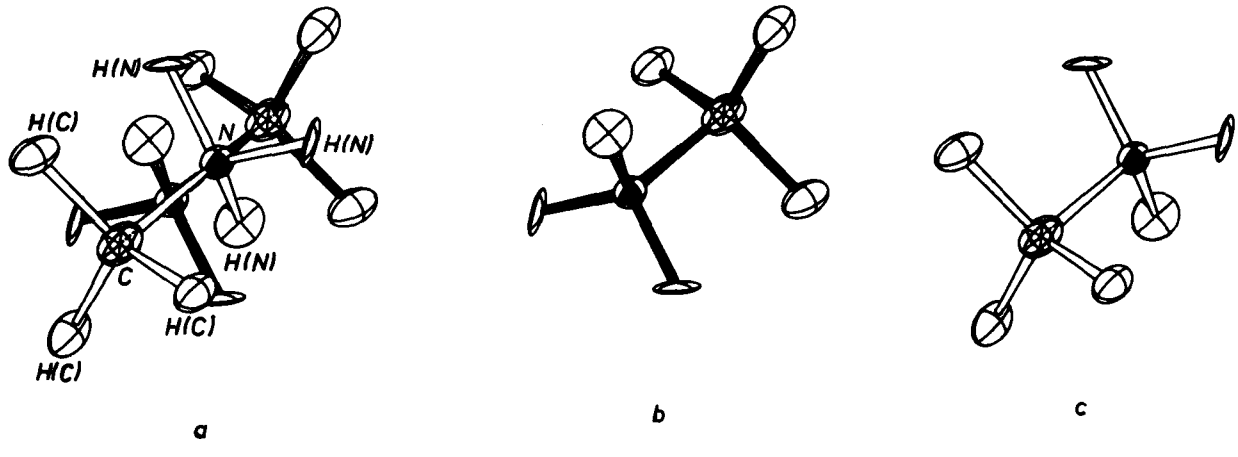

Fig.14. The $(NH_3CH_3)^+$ group centred at the centre of symmetry $(\frac{1}{2}\ \frac{1}{2}\ \frac{1}{2})$.

a) The observed configuration, statistical or dynamical.

b) Only one orientation.

c) The other orientation generated by inversion of 14b at $\frac{1}{2}\ \frac{1}{2}\ \frac{1}{2}$.

The $(SO_4)^{2-}$ group forms an almost perfect tetrahedron as shown in Fig.15 with $O_s(1)$-$O_s(2)$ = 2.353(21)Å and $O_s(2)$-$O_s(2)$ = 2.380(1)Å. The mean distances $<O_s-O_s>$ are 2.367Å . The distances S-$O_s(1)$ and S-$O_s(2)$ are 1.454(12) and 1.448(12)Å respectively with a mean $<$ S-O_s $>$

distance of 1.451Å . The tetrahedron angles $\sphericalangle O_s(1)\text{-}S\text{-}O_s(2)$ and $\sphericalangle O_s(2)\text{-}S\text{-}O_s(2)$ are 108.3(14) and 110.6(13)° respectively with a mean angle $\langle\sphericalangle O_s\text{-}S\text{-}O_s\rangle$ of 109.5°.

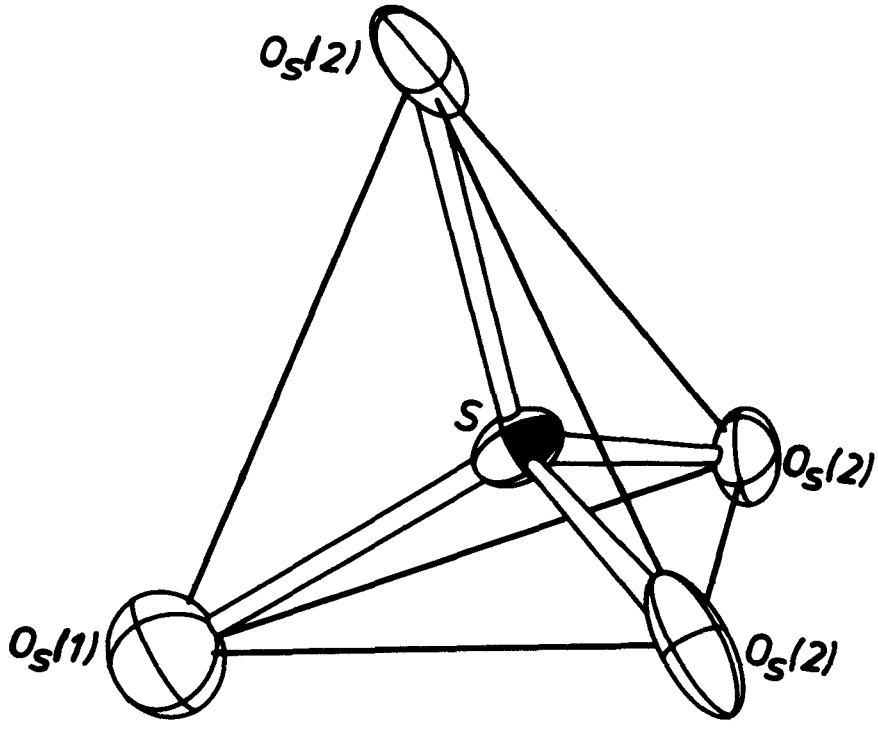

Fig.15. The regular $(SO_4)^{2-}$ tetrahedron.

Large thermal parameters for O_s atoms are observed also for MASD alum, namely B_{equ} = 4.9Å^2 for $O_s(1)$ and B_{equ} = 4.5Å^2 for $O_s(2)$ from neutron data. Therefore a check for possible disorder has been performed. From a three-dimensional difference Fourier map, however no new peaks were observed. The disorder positional parameters of the sulfate oxygen atoms $O_s(1)'$ and $O_s(2)'$ of AASD alum were taken to calculate a disorder structure for MASD alum. The least-squares calculations including a disorder parameter k, with k = 0.05, as starting value led to a disorder of only 0.043(6). More over, when the thermal parameters of these disordered atoms were

refined as anisotropic temperature factors, they became negative. The 4.3% disorder of the oxygen sulfate lies in the range of the R factor (R = 6.4%), therefore there is practically no disorder in MASD alum. The thermal parameters and the R factors without and with disorder are compared and compiled in Table 11.

Table 11. Comparison of thermal parameters and R factors for ordered and disordered (SO_4) groups from neutron data in MASD alum.

		ordered (SO_4) k = 0%	disordered (SO_4) k = 4.3%
	B_{11}	4.9	4.3
$O_s(1)$	B_{12}	0.3	0.2
	B_{equ}	4.9	4.3
	B_{11}	3.5	3.3
	B_{22}	7.2	6.7
	B_{33}	2.9	2.5
$O_s(2)$	B_{12}	-2.6	-2.5
	B_{13}	1.0	0.9
	B_{23}	-3.0	-2.8
	B_{equ}	4.5	4.2
		Agreement values	
	R	0.064	0.063
	$R_{o.u.}$	0.051	0.049
	R_w	0.030	0.029
	$R_{w.o.u.}$	0.029	0.028

o.u. omitting unobserved

6. RESULTS OF $(NH_3OH)Al(SO_4)_2.12H_2O$ ALUM

6.1 Experimental Data

For the neutron diffraction experiments, crystals of HASD alum, $(NH_3OH)Al(SO_4)_2.12H_2O$, were ground to spheres with radii of about 3.0 mm. From the setting of 12 independent reflections the lattice constant was determined by least-squares methods to a = 12.328Å in good agreement with 12.314Å reported by Haussühl /39/. Up to $2\Theta_{max} = 65^\circ$ a total of 2288 reflections was measured in the four octants hkl, $\bar{h}kl$, $h\bar{k}l$ and $hk\bar{l}$. Considering the cubic symmetry, thus each reflection has been measured 12 times. Symmetry related reflections were averaged resulting in a set of 194 unique reflections, of which 39 with $\left[I < 2.0\sigma(I) \right]$ were considered unobserved.

The absorption coefficient for this compound was measured to $\mu = 2.07\ cm^{-1}$ ($\mu R = 0.31$). Absorption correction was consequently considered negligible (transmission = 61.83% for $2\Theta = 0^\circ$ and 62.32% for $2\Theta = 65^\circ$).

6.2 Structure Refinement

Analogous to the technique adopted for the neutron diffraction study of MASD alum, the atomic positions of the skeleton $Al(SO_4)_2.12H_2O$ were used as starting values for a three-dimensional difference Fourier map. Three positive peaks could be recognized on the threefold body diagonal representing N and O, and further 12 negative peaks in the near vicinity indicated the hydrogen positions of the $(NH_3OH)^+$ group. One positive peak lies at the centre of symmetry $\frac{1}{2}\ \frac{1}{2}\ \frac{1}{2}$, the other

two positive peaks on the threefold body diagonal at xxx with x = ± 0.46. From the MASD structure refinement (5.2.2) it is verified that the nitrogen atom occupies the position 4(b) at $\frac{1}{2}\ \frac{1}{2}\ \frac{1}{2}$ and the carbon atom the 8(c) position xxx. In order to prove that in HASD the oxygen atom of the hydroxyl group takes the position of the carbon atom of the methyl group in MASD alum, difference Fourier maps were calculated. Under the assumption of N at xxx with x = 0.46 and O at $\frac{1}{2}\ \frac{1}{2}\ \frac{1}{2}$, three strong density maxima were observed, one positive at $\frac{1}{2}\ \frac{1}{2}\ \frac{1}{2}$ representing the positive difference in the nuclear scattering amplitudes between N and O ($b_N - b_O$ = 9.40 - 5.77 f), and two negative at xxx with x = ± 0.46 representing the negative difference ($b_O - b_N$ = 5.77 - 9.40f). This means that nitrogen lies at the centre of symmetry and oxygen is statistically distributed on two positions on the threefold body diagonal.

The hydrogen H(O) of the hydroxyl group was found to occupy the general position 24(d) with x = 0.52, y = 0.41 and z = 0.43 which implies statistical distribution over six positions around the oxygen atom. Similarly the three hydrogen atoms H(N) were found at 24(d) with x = 0.57, y = 0.53 and z = 0.48 implying statistical distribution over two positions. Fig.16 depicts a section of the difference Fourier map around $\frac{1}{2}\ \frac{1}{2}\ \frac{1}{2}$ with $z \leqq 0.5$ yielding two positive and six negative peaks. This map has to be implemented by inversion at $\frac{1}{2}\ \frac{1}{2}\ \frac{1}{2}$.

The complete crystal structure could then be refined by full-matrix least-squares analysis with isotropic temperature factors to a residual of R = 0.12. By admitting the nitrogen to leave the special $\frac{1}{2}\ \frac{1}{2}\ \frac{1}{2}$ position in favour to the more general 8(c) xxx with x = 0.5 ± 0.013, the R factor decreased to 0.09.

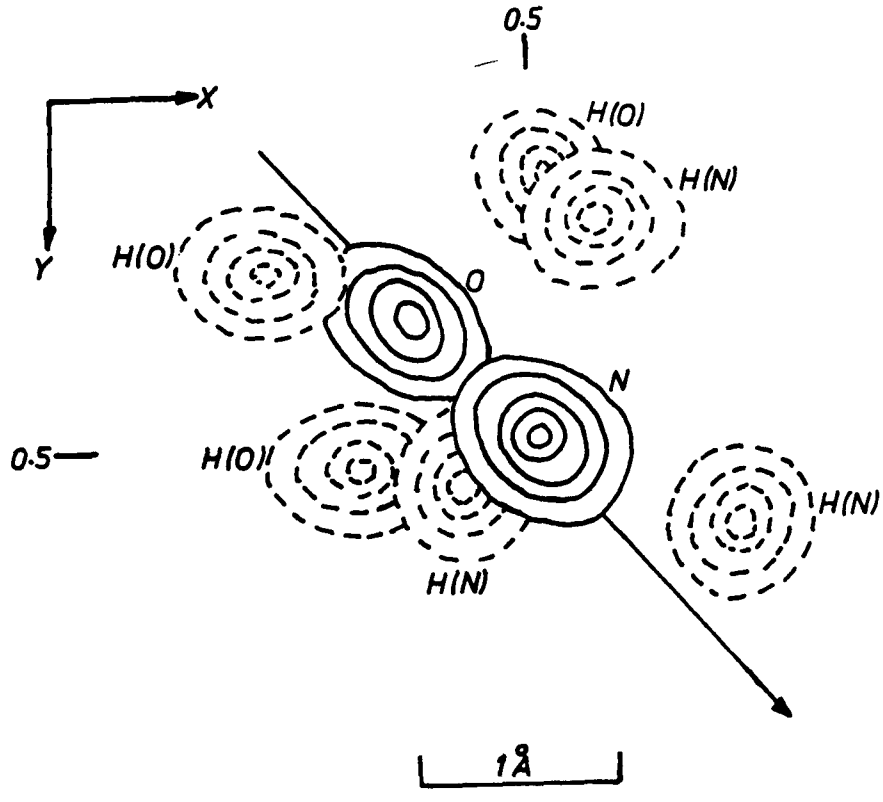

Fig.16. Difference Fourier map around $\frac{1}{2}\ \frac{1}{2}\ \frac{1}{2}$ with $z \leqq 0.5$.

Final refinement was calculated with anisotropic temperature factors for all atoms, including hydrogen, and using the weighting scheme (2.53) with $w = 0.76$ for $|F| \geqq 70$ and $w = 0.00015|F|^2 + 0.00028|F| + 0.001$ for $|F| < 70$. Including an isotropic extinction factor (2.43) in the list of variables (final $g = 2.42(8)\times10^{-5}$) the R_w factor decreased to 0.018. The final atomic and thermal parameters are listed in Tables 12a and 12b respectively. The observed structure amplitudes and the calculated structure factors from parameters of Tables 12a and 12b are tabulated in Table /74/.

Table 12a. Fractional atomic coordinates ($x10^4$) with e.s.d's in parentheses for HASD alum.

Atom	Wyckoff position	Site	Occupancy	x	y	z
Al	4(a)	000	1			
S	8(c)	xxx	1	3022(13)		
$O_s(1)$	8(c)	xxx	1	2328(8)		
$O_s(2)$	24(d)	xyz	1	6913(3)	7526(4)	911(2)
N	8(c)	xxx	1/2	5130(9)		
H(N)	24(d)	xyz	1/2	815(9)	5287(13)	236(16)
O	8(c)	xxx	1/2	4533(17)		
H(O)	24(d)	xyz	1/6	4226(30)	5169(40)	3968(39)
$O_w(1)$	24(d)	xyz	1	8509(2)	9796(2)	186(3)
$O_w(2)$	24(d)	xyz	1	419(3)	1373(3)	2984(2)
H(1)	24(d)	xyz	1	5417(3)	2011(4)	4732(4)
H(2)	24(d)	xyz	1	4137(5)	1837(4)	4525(4)
H(3)	24(d)	xyz	1	2138(4)	4933(5)	1958(5)
H(4)	24(d)	xyz	1	2127(4)	6092(5)	1695(4)

Table 12b. Atomic thermal parameters β_{ij} ($\times 10^4$) with e.s.d's in parentheses B_{equ} is included for comparison with previous investigations.

Atom	β_{11}	β_{22}	β_{33}	β_{12}	β_{13}	β_{23}	B_{equ}
Al	47(13)			0			2.9
S	52(14)			2(17)			3.2
$O_s(1)$	107(9)			8(12)			6.5
$O_s(2)$	72(4)	141(4)	68(4)	-38(3)	16(3)	-54(3)	5.7
N	58(12)			1(9)			3.5
H(N)	27(12)	127(21)	220(28)	10(12)	34(16)	-1(12)	7.6
O	100(13)			-48(13)			6.1
H(O)	146(25)	169(29)	170(33)	-4(29)	-44(24)	159(28)	9.8
$O_w(1)$	31(3)	48(4)	53(5)	-3(3)	17(3)	4(3)	2.7
$O_w(2)$	44(4)	81(3)	48(3)	7(4)	-14(2)	-3(2)	3.5
H(1)	36(6)	68(6)	51(6)	-2(5)	3(5)	1(5)	3.1
H(2)	80(7)	53(5)	60(5)	7(5)	9(6)	7(5)	3.9
H(3)	93(8)	99(6)	70(7)	-15(6)	28(5)	14(6)	5.3
H(4)	92(7)	99(8)	77(6)	21(6)	11(5)	-4(6)	5.4

Separate refinement calculations were performed for the hkl, lhk and klh reflection sets averaged over the 4-octants and in addition for the mean values of all measured reflections. Comperative results for all refinements are listed in Table 13.

Table 13. Comparison between R factors, secondary extinction coefficient and goodnes of the fit for < hkl> , < lhk> , < klh > , < all reflections> and < unique reflections > .

	< hkl>	< lhk>	< klh>	< all refle.>	< unique refle.>
R	0.065	0.071	0.066	0.071	0.054
$R_{o.u.}$	0.043	0.047	0.041	0.049	0.037
R_w	0.021	0.025	0.022	0.031	0.019
$R_{w.o.u.}$	0.020	0.024	0.020	0.030	0.018
g x 10^{-5}	3.0(3)	2.6(2)	2.7(2)	2.5(2)	2.4(1)
goodnes of fit	1.064	1.224	1.102	1.243	0.942

o.u. omitting unobserved

6.3 Discussion of the Structure

The HASD alum is characteristic of the α-alum type like AASD and MASD alums. A projection of the complete structure with only one orientation of the $(NH_3OH)^+$ group is depicted in Fig.17 (only one half of the unit cell is shown). Six water molecules $H_2O_w(1)$ surround each

aluminium ion in the form of a regular octahedron as shown in Fig.17. The Al-$O_w(1)$ distances are 1.868(2)Å. The $O_w(1)$-$O_w(1)$ distances are 2.649(1) and 2.631(5)Å with a mean $<O_w(1)-O_w(1)>$ distance of 2.640Å.

The $(NH_3OH)^+$ group is coordinated by the other six water molecules in the form of a highly distorted octahedron like in AASD and MASD alums. The nearest distances of $O_w(2)$ to $O_w(2)$ are 3.321(1)Å. These six water molecules around the $(NH_3OH)^+$ group can be separated into two groups of three each as in the other two alums. The distances of the nitrogen and oxygen atoms of the $(NH_3OH)^+$ group to the nearest $O_w(2)$ atoms are 2.994(3) and 2.966(2)Å respectively. The distances of the H(N) and H(O) atoms to the nearest $O_w(2)$ atoms are 2.045(20) and 1.970(24)Å respectively.

The $(NH_3OH)^+$ group itself is difficult to visualize. Fig.18a depicts the idealized configuration. In Fig.18b we have applied the threefold rotation symmetry of [111], which is the line N-O. In order to have the true observed structure, a centre of symmetry must be introduced yielding Fig.18c. The N-O distance along [111] is 1.282(17)Å.

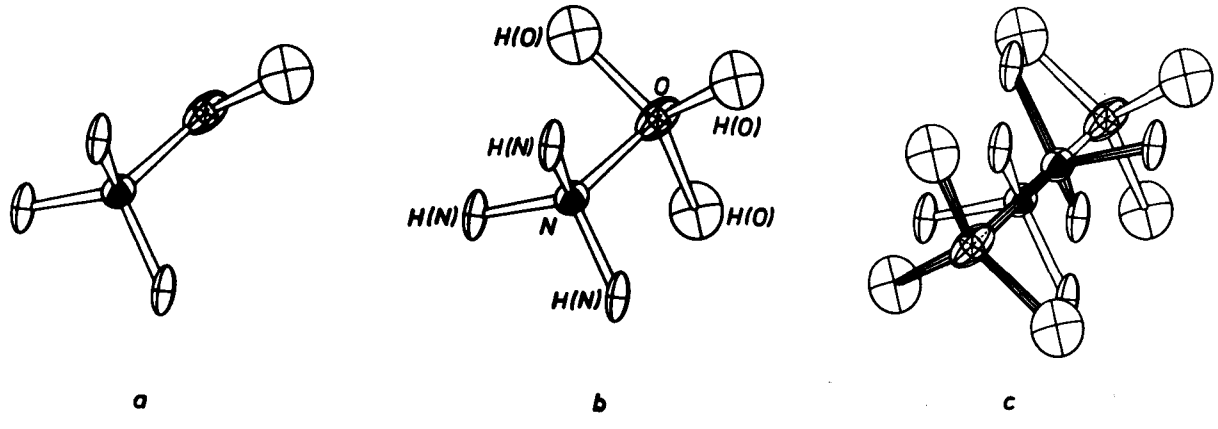

Fig.18. The $(NH_3OH)^+$ group.

a) in idealized configuration.
b) with the threefold rotational symmetry of [111].
c) with the centre of symmetry at $\frac{1}{2}\ \frac{1}{2}\ \frac{1}{2}$.

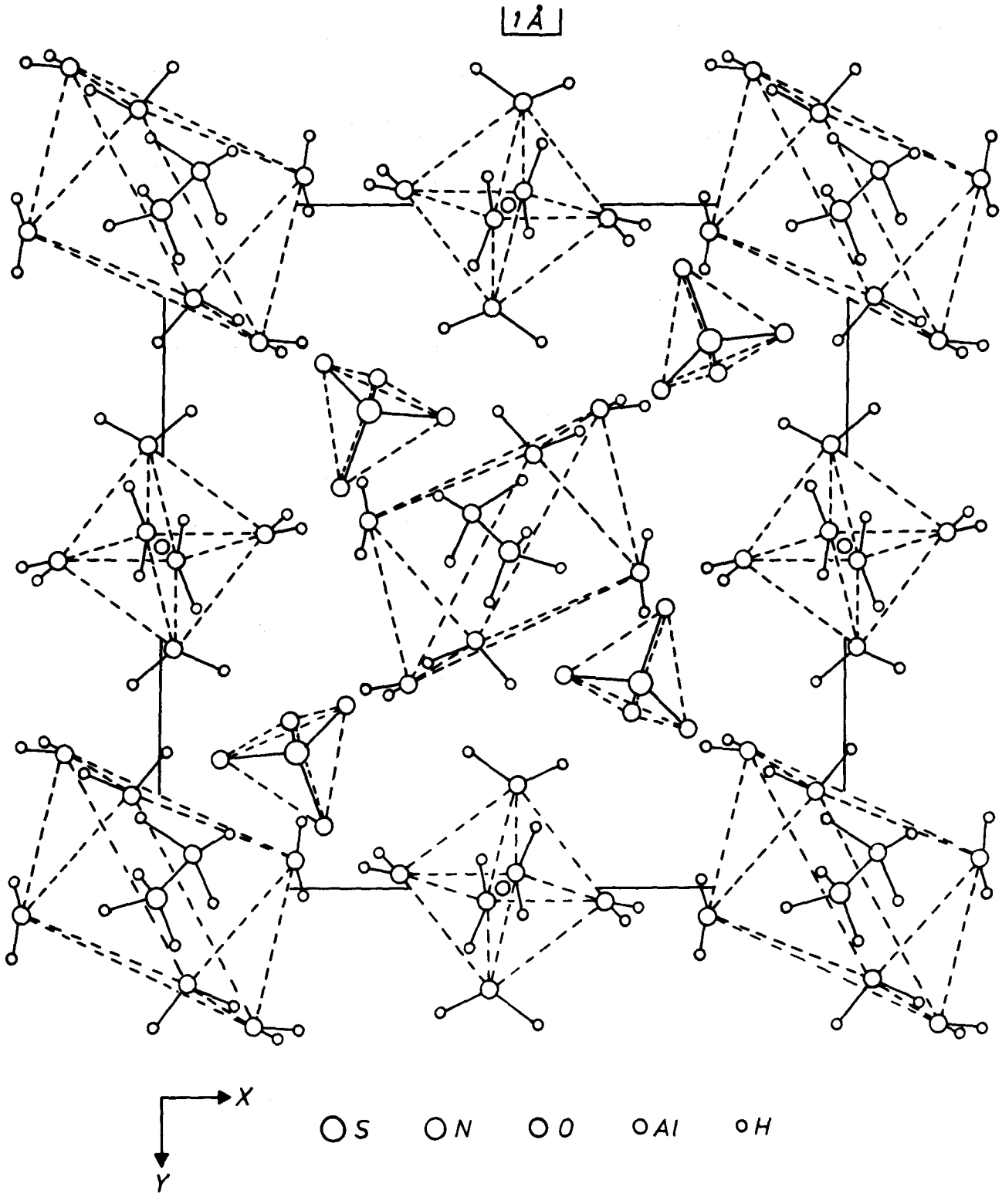

Fig.17. Projection on the xy-plane of the HASD alum ($0.2 \leqq z \leqq 0.7$).
[For simplicity only one orientation of the (NH_3OH) group is shown].

Unusually large thermal parameters have been observed for the hydrogen atoms of the $(NH_3OH)^+$ group namely $B_{equ} = 7.6\text{Å}^2$ for H(N) and $B_{equ} = 9.8\text{Å}^2$ for H(O). Similar values have also been observed in hydroxylammonium perchlorate, $(NH_3OH)ClO_4$, by Prince, Dickens and Rush /72/ with mean values of B_{equ} for H(N) and H(O) of 7.8 and 7.0Å^2 respectively.

The $(SO_4)^{2-}$ group forms an almost perfect tetrahedron. The distances are $S\text{-}O_s(1) = 1.482(10)$Å and $S\text{-}O_s(2) = 1.452(13)$Å and the mean $< O_s\text{-}O_s >$ distances are 2.383Å.

Large thermal parameters have also been found for the sulfate oxygen atoms namely $B_{equ} = 6.5\text{Å}^2$ for $O_s(1)$ and $B_{equ} = 5.7\text{Å}^2$ for $O_s(2)$. An attempt has been made to refine a disorder structure with additional sulfate oxygen atoms, as in the case of MASD alum, by including a disorder parameter k in the list of variables. The least-squares analysis led to a disorder of only 3%. This means that there is practically no disorder in this compound. The thermal parameters and R factors without and with disorder are compared and compiled in Table 14.

Table 14. Comparison of thermal parameters and R factors for ordered and disordered (SO_4) groups in HASD alum.

		ordered (SO_4) k = 0%	disordered (SO_4) k = 3%
	B_{11}	6.5	6.1
$O_s(1)$	B_{12}	0.5	0.3
	B_{equ}	6.5	6.1
	B_{11}	4.4	4.3
	B_{22}	8.6	8.4
	B_{33}	4.1	3.9
$O_s(2)$	B_{12}	-2.3	-2.3
	B_{13}	1.0	0.9
	B_{23}	-3.3	-3.2
	B_{equ}	5.7	5.5
		Agreement values	
	R	0.054	0.052
	$R_{o.u.}$	0.037	0.036
	R_{w}	0.019	0.018
	$R_{w.o.u.}$	0.018	0.017

o.u. omitting unobserved

7 COMPARISON OF THE RESULTS OF THE THREE ALUMS

The three AASD, MASD and HASD alums are characteristic of the α-alum type. As in all alums there are 12 water molecules surrounding the monovalent and the trivalent cations.

The six water molecules $H_2O_w(1)$ around each aluminium ion lie on the corners of an almost regular octahedron with mean distances and angles from the three alums of $< O_w(1)-O_w(1) > = 2.647$Å, $< Al-O_w(1) > = 1.872$Å and $< \sphericalangle O_w(1)-Al-O_w(1) >$ of 90.5° and 89.5°. Within the water molecules we find $< O_w(1)-H(1) > = 0.994$Å, $< O_w(1)-H(2) > = 0.995$Å and $< \sphericalangle H(1)-O_w(1)-H(2) > = 107.6^\circ$ with a mean $< O_w(1)-H >$ value of 0.994Å. Table 15 lists a comparison between the distances and angles of this octahedron in the three alums.

Table 15. Comparison between Al-$6H_2O$ octahedra in AASD, MASD and HASD alums.

	AASD	MASD	HASD
		distances in (Å)	
Al-$O_w(1)$	1.897(2)	1.851(5)	1.868(2)
$O_w(1)-O_w(1)$	2.693(1)	2.634(8)	2.649(5)
$O_w(1)-O_w(1)$	2.671(5)	2.602(7)	2.631(5)
$< O_w(1)-O_w(1) >$	2.682	2.618	2.640
$O_w(1)-H(1)$	0.989(9)	1.007(2)	0.986(9)
$O_w(1)-H(2)$	0.960(4)	1.029(12)	0.995(5)
H(1)-H(2)	1.571(1)	1.630(5)	1.612(1)
$< O_w(1)-H >$	0.975	1.018	0.991
		angles in degree	
$O_w(1)-Al-O_w(1)$	90.5(1)	90.7(1)	90.3(2)
$O_w(1)-Al-O_w(1)$	89.5(1)	89.3(1)	89.7(2)
$H(1)-O_w(1)-H(2)$	107.4(1)	106.4(5)	109.0(6)

The other six water molecules $H_2O_w(2)$ are surrounding the monovalent cation in the form of distorted octahedron in the three alums. These water molecules can be separated into two groups $H_2O_w(2)$ and $H_2O_w(2')$ of three each. The important distances and angles of these distorted octahedra are given in Table 16.

Table 16. Comparison between distances and angles of the M^+ groups with the surrounding six water molecules in AASD, MASD and HASD alum

	AASD	MASD	HASD
		distances in (Å)	
N-$O_w(2)$	2.990(3)	2.994(1)	2.994(1)
N-$O_w(2')$	3.065(5)	3.159(1)	3.132(3)
C-$O_w(2)$		3.481(45)	
C-$O_w(2')$		2.979(7)	
O-$O_w(2)$			3.440(19)
O-$O_w(2')$			2.966(2)
<N-$O_w(2)$>	3.028	3.077	3.063
<C-$O_w(2)$>		3.230	
<O-$O_w(2)$>			3.203
$O_w(2)$-H(3)	0.953(1)	0.929(2)	0.950(1)
$O_w(2)$-H(4)	0.984(2)	0.945(3)	0.934(4)
H(3)-H(4)	1.543(7)	1.465(2)	1.465(1)
<$O_w(2)$-H>	0.969	0.937	0.942
		angles in degree	
$O_w(2)$-N-$O_w(2)$	115.8(2)	117.9(1)	117.5(2)
$O_w(2')$-N-$O_w(2')$	111.5(3)	108.7(1)	109.6(3)
$O_w(2)$-C-$O_w(2)$		95.0(17)	
$O_w(2')$-C-$O_w(2')$		119.0(5)	
$O_w(2)$-O-$O_w(2)$			96.2(7)
$O_w(2')$-O-$O_w(2')$			119.3(2)
<$O_w(2)$-N-$O_w(2)$>	113.7	113.3	113.6
<$O_w(2)$-C-$O_w(2)$>		107.0	
<$O_w(2)$-O-$O_w(2)$>			107.8
H(3)-$O_w(2)$-H(4)	105.6(5)	102.8(5)	102.4(4)

The mean distances between the nitrogen atom of the monovalent cation and the oxygen $O_w(2)$ and $O_w(2')$ of the water molecules are 2.993 and 3.119Å respectively. The mean of the nearest distance between the $O_w(2)$ atoms is 3.319Å. Here we find for the mean values of the water molecules: $< O_w(2)\text{-}H(3) > = 0.954$Å and $< O_w(2)\text{-}H(4) > = 0.949$Å and $< \sphericalangle H(3)\text{-}O_w(2)\text{-}H(4) > = 103.6^{\circ}$ with a mean value of $< O_w(2)\text{-}H >$ of 0.949Å.

The different configurations of the monovalent cation, the hydrogen bonding system and the behaviour of the (SO_4) groups in the three alums are discussed below in Chapters 8,9 and 10 respectively.

8. DIFFERENT CONFIGURATIONS OF THE (NH_3-H), (NH_3CH_3) AND (NH_3OH) GROUPS

The structures derived in this study exhibit partial occupancies of crystallographic sites for NH_4, (NH_3CH_3) and (NH_3OH) group atoms. This requires further discussion and attention. Three possible models will be discussed where finaly only one can explain all experimental findings. A comparison between the distances and angles in the three groups is given in Table 17.

Table 17. Comparison between distances and angles of M^+ groups in AASD, MASD and HASD alums.

	AASD	MASD	HASD
		distances in (Å)	
N-C		1.397(84)	
N-O			1.282(17)
N-H_N(1)	1.150(11)		
N-H_N(2)	0.911(10)		
N-H(N)		1.026(23)	0.978(14)
C-H(C)		1.159(4)	
O-H(O)			1.113(1)
		angles in degree	
H_N(1)-N-H_N(2)	115.3(4)		
H_N(2)-N-H_N(2)	103.1(14)		
C-N-H(N)		108.5(3)	
O-N-H(N)			110.6(12)
H(N)-N-H(N)		110.4(3)	108.3(12)
H(C)-C-H(C)		112.7(11)	
H(O)-O-H(O)			117.8(22)
N-C-H(C)		106.0(14)	
N-O-H(O)			98.5(48)

8.1 Domain Model (Fig.19a)

The physical properties of these alums require centrosymmetry which contradicts the Eigensymmetrie of the three groups. The centrosymmetry can be reached for the whole crystal for example by doubling at least one axis of the unit cell and reversing NH_3 and $H_N(1)$ (AASD), NH_3 and CH_3 (MASD), NH_3 and OH (HASD) in the second unit cell. This domain model is depicted in Fig.19a with two axes being doubelled. The NH_3 group is represented by dots and $H_N(1)$, CH_3 and OH by circles. This model would require superstructure reflections, which have not been observed. In fact any equal distributions A and B within one mosaic block would lead to the observed structure, since only the space-average structure can be observed with the chosen unit cell. This leads directly to the statistical model.

8.2 Statistical Model (Fig.19b)

In this model a statistical distribution was assumed over the more general positions 8(c) and 24(d). Only one half of the positions of the (NH_3-H) and (NH_3CH_3) group atoms are occupied while one half of N,O and H(N) and 1/6 of the sites of H(O) in the (NH_3OH) group are occupied in this picture. In this space-average picture again a single unit cell has no centre of symmetry in the case of HASD alum only, but the whole crystal exhibits centrosymmetry. Such a statistical arrangement has been infered for the (NH_3OH) group from infrared data by Acharya and Narayanan /73/ in a study of $(NH_3OH)Al(SO_4)_2.12H_2O$ alum.

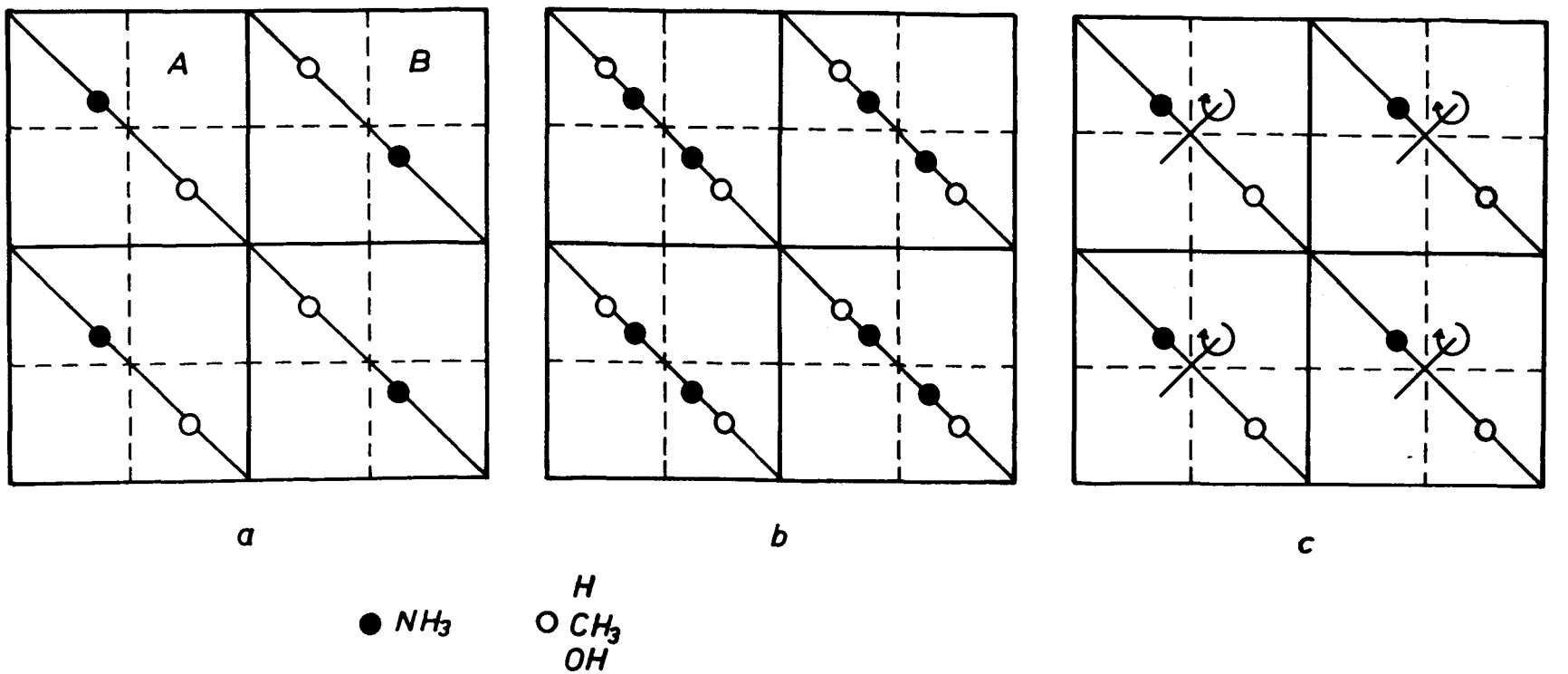

Fig.19. Different configurations of the (NH_3-H), (NH_3CH_3) and (NH_3OH) groups

a) Domain model. b) Statistical model. c) Dynamical model.

8.3 Dynamical Model (Fig.19c)

With elastic neutron diffraction, i.e., without energy analysis of the diffracted beam, a differentiation between statistical and dynamical models cannot take place, this means between space and time-average. Models 19a and 19b are both space-average models. A model has to be selected , which allows a quantized rotation of the three groups around an axis perpendicular to [111]. This model is depicted in Fig.19c. It gives the same observational data as the other two models, and cannot be separated from the other models by elastic neutron diffraction or X-ray alone. However, from the NMR measurements such a behaviour is to be favoured. This model has been proposed for example by Weiden and Weiss/30/ for $(NH_3NH_2)Al(SO_4)_2.12H_2O$ alum by analysing the NMR-spectra. According to this model the $(NH_3NH_2)^+$ group performs a hindered or free rotation perpendicular to the N-N bond with a frequency of $\approx 10^6$ Hz ($\approx 10^{-6}$ sec.). This rotation is too fast for elastic neutron diffraction or X-ray and will result in a time-average picture, i.e., in agreement with our findings. We belive the same behaviour to occure for the three alums and therefore we conclude that the $(NH_3\text{-}H)^+$, $(NH_3CH_3)^+$ and $(NH_3OH)^+$ group atoms have an analogous dynamical behaviour.

9 HYDROGEN BRIDGES

The alum structure is held together by a system of hydrogen bonds between the water molecules and between the water molecules and the sulfate oxygen atoms. This means between $O_w(1)$ and $O_w(2)$ and between O_w and O_s. A survey of the hydrogen bridges is depicted in Fig.20. The interatomic distances and angles for the hydrogen bond system are given in Table 18.

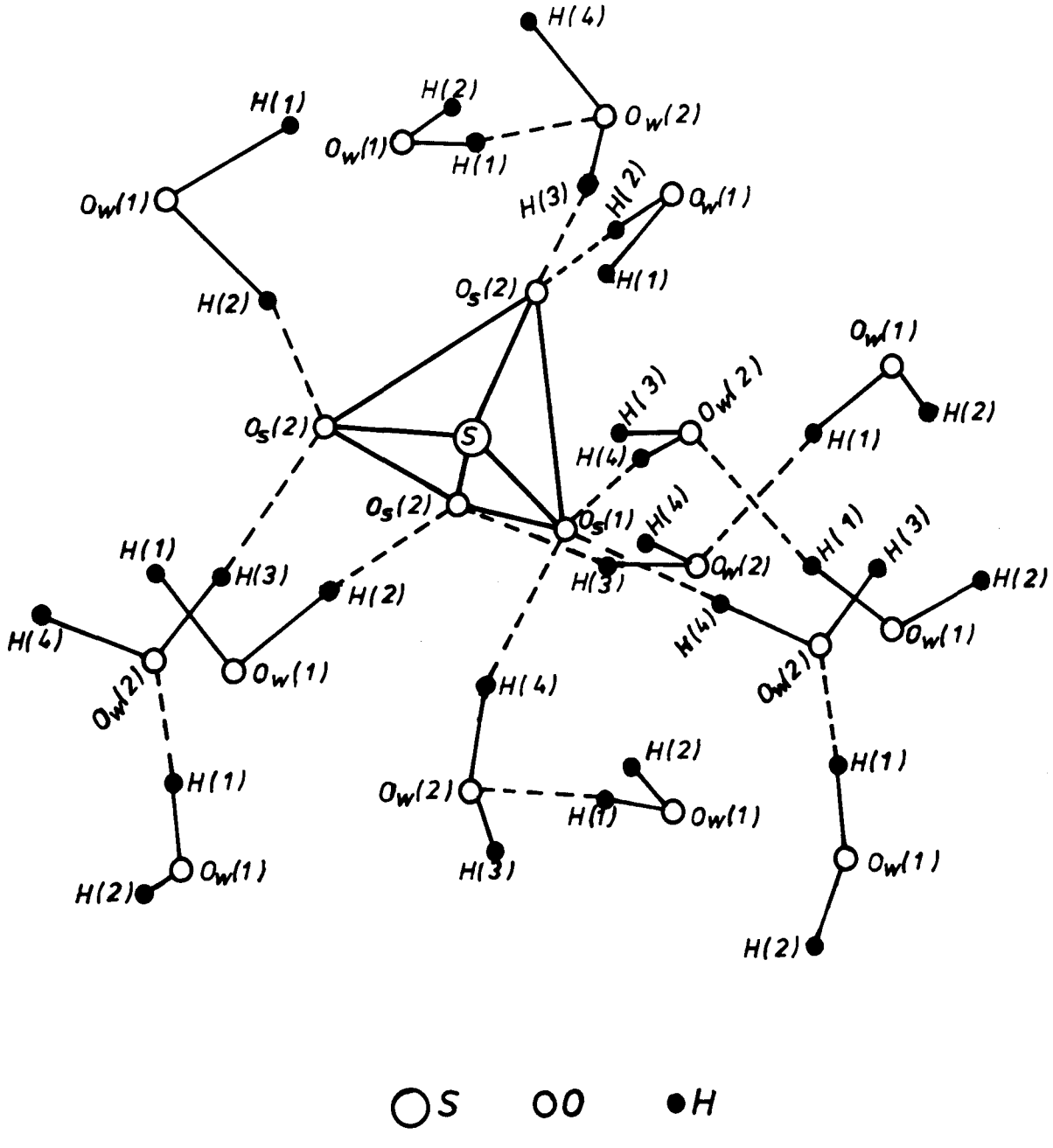

Fig.20. The system of the hydrogen bonds (broken lines).

The two hydrogen atoms belonging to the water molecules $H_2O_w(1)$ coordinated to an aluminium ion form two unequal hydrogen bonds, one H(1) to an oxygen atom $O_w(2)$ of the water molecules (not coordinated to an aluminium), with a hydrogen bond of a mean length for the three alums of $< O_w(2)\text{-}H(1) > = 1.663$Å and a mean angle $< \sphericalangle O_w(1)\text{-}H(1)\text{-}O_w(2) > = 175.9^\circ$. The other hydrogen atom H(2) is bonded to an oxygen atom $O_s(2)$ of the sulfate group with a hydrogen bond of a mean length of 1.633Å with $< \sphericalangle O_w(1)\text{-}H(2)\text{-}O_s(2) > = 173.2^\circ$. The other two hydrogen atoms of an oxygen $O_w(2)$ form two hydrogen bonds, one H(3) to an oxygen $O_s(2)$ of the sulfate group with a hydrogen bond of a mean length of $< O_s(2)\text{-}H(3) > = 1.814$Å and $< \sphericalangle O_w(2)\text{-}H(3)\text{-}O_s(2) > = 172.2^\circ$, the other hydrogen atom H(4) to an oxygen atom $O_s(1)$ with a hydrogen bond of a mean length of $< O_s(1)\text{-}H(4) > = 1.836$Å with $< \sphericalangle O_w(2)\text{-}H(4)\text{-}O_s(1) > = 165.5^\circ$. Since this oxygen atom lies on a threefold axis, it is bonded simultaneously to three H(4) atoms.

In the case of AASD alum, there are additional hydrogen bonds, namely $O_s(2')\text{-}H(2) = 2.08(3)$Å with $\sphericalangle O_w(1)\text{-}H(2)\text{-}O_s(2') = 156(1)^\circ$ and $O_s(2')\text{-}H(3) = 2.02(2)$Å with $\sphericalangle O_w(2)\text{-}H(3)\text{-}O_s(2') = 157(1)^\circ$.

The hydrogen atoms H(2), H(3) and the atoms S, $O_s(2)$ of the sulfate group are nearly coplanar, with $O_s(2)$ being < 0.14Å$>$ out of the plane through S, H(2) and H(3). The mean sum of the angles around $O_s(2)$ is 358°.

Table 18. Comparison between the hydrogen bonding system in AASD, MASD and HASD alums.

hydrogen bridges A—B····C	distances in (Å) AASD	MASD	HASD	angles in degree AASD	MASD	HASD
$O_w(1)$—H(1)····$O_w(2)$				$O_w(1)$-H(1)-$O_w(2)$		
$O_w(1)$—H(1)	0.989(1)	1.007(2)	0.986(9)			
$O_w(1)$—$O_w(2)$	2.616(6)	2.677(6)	2.674(8)	176.4(1)	176.3(11)	175.0(1)
$O_w(2)$····H(1)	1.628(2)	1.671(9)	1.690(2)			
$O_w(1)$—H(2)····$O_s(2)$				$O_w(1)$-H(2)-$O_s(2)$		
$O_w(1)$—H(2)	0.960(4)	1.029(12)	0.995(5)			
$O_w(1)$—$O_s(2)$	2.593(1)	2.654(8)	2.631(5)	171.1(6)	174.3(12)	174.2(8)
$O_s(2)$····H(2)	1.640(2)	1.620(3)	1.639(9)			
$O_w(1)$—H(2)····$O_s(2)'$				$O_w(1)$-H(2)-$O_s(2)'$		
$O_w(1)$—$O_s(2)'$	2.99(3)					
$O_s(2)'$····H(2)	2.08(3)			156(1)		
$O_w(2)$—H(3)····$O_s(2)$				$O_w(2)$-H(3)-$O_s(2)$		
$O_w(2)$—H(3)	0.953(1)	0.929(2)	0.950(1)			
$O_w(2)$—$O_s(2)$	2.758(2)	2.749(2)	2.748(1)	170.4(4)	173.1(11)	173.1(6)
$O_s(2)$····H(3)	1.814(2)	1.824(1)	1.803(2)			
$O_w(2)$—H(3)····$O_s(2)'$				$O_w(2)$-H(3)-$O_s(2)'$		
$O_w(2)$—$O_s(2)'$	2.92(2)					
$O_s(2)'$····H(3)	2.02(2)			157(1)		
$O_w(2)$—H(4)····$O_s(1)$				$O_w(2)$-H(4)-$O_s(1)$		
$O_w(2)$—H(4)	0.972(2)	0.945(3)	0.934(4)			
$O_w(2)$—$O_s(1)$	2.786(8)	2.764(7)	2.753(7)	160.7(1)	168.9(12)	167.0(9)
$O_s(1)$····H(4)	1.838(6)	1.831(1)	1.838(1)			
	mean distances			mean angles		
<A—B>	0.984	0.978	0.966			
<A—C>	2.688	2.711	2.966	169.7	173.2	172.3
<B····C>	1.730	1.737	1.743			

10 THE BEHAVIOUR OF THE SULFATE GROUPS

Since the completion of alum structure investigations by Lipson and Beevers /40/ and Lipson /56/, interest in the various properties of these double salts has continued and much attention has been attracted to the anomalous behaviour of the sulfate groups. In order to conform to the space group Pa3 to which the alums belong, each sulfate group is oriented with the sulfur and one oxygen atom $O_s(1)$ in special positions on the threefold axis and with the remaining three oxygen $O_s(2)$ in general positions around this axis.

The oxygen atoms, and in particular those on the threefold axis have unusually large thermal parameters. These values have been found previously in several of the alums which have been studied in sufficient detail: Bacon and Gardner /57/ found B = 8.0 and 6.9$Å^2$ in $KCr(SO_4)_2.12H_2O$; Larson and Cromer /44/ found B = 7.0 and 4.4$Å^2$ in $RbAl(SO_4)_2.12H_2O$ and B = 13.0 and 7.0$Å^2$ in $KAl(SO_4)_2.12H_2O$ for $O_s(1)$ and $O_s(2)$ respectively.

In this study, some degree of disorder in the localizatior of the sulfate groups was introduced to explain the anomalous behaviour of the sulfate groups. This disorder was introduced by the inversion of a certain fraction of the sulfate groups along the threefold axis. In the AASD alum we found 17% of those disordered sulfate groups, while in the MASD and HASD alums this disorder effect was negligible. The distances and angles of the sulfate groups are compared in Table 19 for the three alu

Another possible explanation for the unusually large thermal parameters of the O_s atoms in MASD and HASD alums may be due to

Table 19. Comparison between the (SO_4) tetrahedra in AASD, MASD and HASD alums.

	AASD	MASD	HASD
ordered group		distances in (Å)	
$S-O_s(1)$	1.539(5)	1.454(12)	1.482(10)
$S-O_s(2)$	1.452(7)	1.448(12)	1.452(13)
$O_s(1)-O_s(2)$	2.423(12)	2.353(21)	2.376(18)
$O_s(2)-O_s(2)$	2.388(1)	2.380(1)	2.390(8)
$<S-O_s>$	1.496	1.451	1.467
$<O_s-O_s>$	2.406	2.367	2.383
		angles in degree	
$O_s(1)-S-O_s(2)$	108.2(7)	108.3(14)	108.1(14)
$O_s(2)-S-O_s(2)$	110.7(7)	110.6(13)	110.8(9)
$O_s(2)-O_s(1)-O_s(2)$	59.1(2)	60.7(6)	60.4(3)
$O_s(2)-O_s(2)-O_s(1)$	60.5(2)	59.6(3)	59.8(1)
$O_s(2)-O_s(2)-O_s(2)$	60.0	60.0	60.0
$<O_s-S-O_s>$	109.5	109.5	109.5
$<O_s-O_s-O_s>$	59.9	60.1	60.1
disordered group	distances in (Å)		
$S-O_s(1)'$	1.52(6)		
$S-O_s(2)'$	1.39(1)		
$O_s(1)'-O_s(2)'$	2.47(4)		
$O_s(2)'-O_s(2)'$	2.18(2)		
$<S-O_s'>$	1.46		
$<O_s'-O_s'>$	2.33		
	angles in degree		
$O_s(1)'-S-O_s(2)'$	115.5(8)		
$O_s(2)'-S-O_s(2)'$	102.8(10)		
$O_s(2)'-O_s(1)'-O_s(2)'$	52.3(4)		
$O_s(2)'-O_s(2)'-O_s(1)'$	63.9(1)		
$O_s(2)'-O_s(2)'-O_s(2)'$	60.0		
$<O_s'-S-O_s'>$	109.2		
$<O_s'-O_s'-O_s'>$	58.7		

a simultaneous oscillation of the S and $O_s(1)$ atoms with equal probability around any one of the three axes passing through the sulfur atom and each of the three oxygen atoms $O_s(2)$ in general positions as stated by Steeple et al. /38/. This study suggests roughly the same magnitude of oscillation for all alums. According to our different findings for the AASD, MASD and HASD alums we believe in a type-dependent anomaly of the sulfate group localizations.

11 REFERENCES

/1/ Kraus,D.L. and Nutting,G.C.: J. Chem. Phys. 9, 133 (1941).

/2/ Couture,L., Jacquinot,P. and Tsujikawa,I.: Conference on low temperature crystallography, Oxford, April 1956; Brit. J. Appl. Phys. 7, 434 (1956).

/3/ Benzie,R.J. and Cooke,A.H.: Proc. Phys. Soc. (London), A63, 213 (1950).

/4/ Johnston,H.J., Hu, J.H. and Horton,W.S.: J. Am. Chem. Soc. 75, 3922 (1953).

/5/ Haussühl,S. and Trost,F.: Z. Naturforsch. 14a, 437 (1959).

/6/ Haussühl,S.: Z. Krist. 111, 321 (1959).

/7/ Buck,P. and Haussühl,S.: Optic 24, 146 (1967).

/8/ Weber,H.J. and Haussühl,S.: Phys. Stat. Sol. (b)65, 633 (1974).

/9/ Weber,H.J. and Haussühl,S.: Acta Cryst. A32, 892 (1976).

/10/ Guillien,R.: Compt. rend. 209, 21 (1939), 213, 991 (1941).; Cahiers Phys. 11, 17 (1942).

/11/ Garnier,J.: Les Diélectriques, Dunod, Paris (1948).

/12/ Freymann,M., Rolland,M.T. and Freymann,R.: Comp. rend, 232, 2312 (1951).

/13/ Griffiths,J.H.E. and Powell,J.A.: Proc. Phys. Soc. (London), A65, 289 (1952).

/14/ Eisenstein,J.: Revs. Modern Phys. 24, 74 (1952).

/15/ Pepinsky,R., Jona,F. and Shirane,G.: Phys. Rev. 102, 1181 (1956).

/16/ Jona,F. and Shirane,G.: Ferroelectric Crystal. "International Series of Monographson, Solid State Physics" Vol.I p.324 (1962).

/17/ Hoshino,R.: J. Phys. Soc. Japan 16, 835 (1961).

/18/ O'Reilly,D.E. and Tsong,T.: Phys. Rev. 157, 417 (1967).

/19/ Burns,G.: Phys. Rev. 123, 64 (1961).

/20/ Gronde,S.: Colloque Ampère XIV, 403, (1967) North-Holland Publ. Co.

/21/ Pfiffer,H.: Z. angew. Physik 6, 508 (1955).

/22/ Segleken,W.G. and Torrey,H.C.: Phys. Rev. 98, 1537 (1955).

/23/ Vinogradova, I.S.: Sov. Phys. Solid State 10, 727 (1969).

/24/ Vinogradova,I.S. and Falaleeva,L.G.: Bull. Acad. Sci. USSR 33, 231 (1969).

/25/ Burns,G.: J. Chem. Phys. 32, 1585 (1960).

/26/ Story,H.S., Bailey,W. and Kline,D.: Bull. Amer. Phys. Soc. 13, 885 (1968).

/27/ Weiden,N. and Weiss,A.: Z. Krist. 134, 475 (1971).

/28/ Bailey,W.C. and Story,H.S.: J. Chem. Phys. 58, 1255 (1973).

/29/ Weiden,N. and Weiss,A. Ber. Bunsenges. physik. Chem. 78, 103 (1974).

/30/ Weiden,N. and Weiss,A. Ber. Bunsenges. physik. Chem. 79, 557 (1975).

/31/ Bendt,P.J.: Phys. Rev. B 2, 4366 (1970).

/32/ Danilov,A.G. and Manoogian,A.: Phys. Rev. B 6, 4097 (1972).

/33/ Danilov,A.G., Vial,J.C. and Manoogian,A.: Phys. Rev. B 8, 3124 (1973).

/34/ Nicula,A., Farcas,S.I. and Darabant?a.: Proc. XVIII. Congress Ampere, Nottingham p.131 (1974).

/35/ Bagguley,D.M.S. and Grifths,J.H.E.: Proc. Roy. Soc. A204, 188 (1950).

/36/ Farcas,S.I., Darabant,A. and Nicula,A.: Phys. Stat. Sol. (b) 74, 335 (1976).

/37/ Gudy,G.: Rev. Chem. Min. 1, 297 (1964).

/38/ Ledsham,A.H.C., Steeple,H. and Hughes,W.: Acta Cryst. B26, 1240 (1970).

/39/ Haussühl,S.: Z. Krist. 116, 371 (1961).

/40/ Lipson,H. and Beevers,C.A.: Proc. Roy. Soc. A148, 664 (1935).

/41/ Okaya,Y., Ahmed,M.S., Pepinsky,R. and Vand,V.: Z. Krist. 109, 367 (1957).

/42/ Cromer,D.T., Kay,M.I. and Larson,A.C.: Acta Cryst. 22, 182 (1967).

/43/ Cromer,D.T., Kay,M.I. and Larson,A.C.: Acta Cryst. 21, 383 (1966).

/44/ Larson,A.C. and Cromer,D.T.: Acta Cryst. 22, 793 (1967).

/45/ Cromer,D.T. and Kay,M.I.: Acta Cryst. 22, 800 (1967).

/46/ Lipson,H.: Phil. Mag. 19, 887 (1935).

/47/ Fletcher,R.O.W. and Steeple,H.: Acta Cryst. 14, 891 (1961).

/48/ Fletcher,R.O.W. and Steeple,H.: Acta Cryst. 15, 960 (1962).

/49/ Fletcher,R.O.W. and Steeple,H.: Acta Cryst. 17, 290 (1964).

/50/ Kozhin,V.M. and Zaitseva,M.P.: Sov. Phys. Cryst. 14, 277 (1969).

/51/ Ledsham,A.H.C. and Steeple,H.: Acta Cryst. B24, 1287 (1968).

/52/ Klug,H.P.: J. Amer. Chem. Soc. 62, 2992 (1940).

/53/ Ledsham,A.H.C. and Steeple,H.: Acta Cryst. B25, 398 (1969).

/54/ Ledsham,A.H.C. and Steeple,H.: Acta Cryst. B24, 320 (1968).

/55/ Sugusch,J.: Acta Cryst. B30, 662 (1974).

/56/ Lipson,H.: Proc. Roy. Soc. A151, 347 (1935).

/57/ Bacon,G.E. and Gardener,W.E.: Proc. Roy. Soc. A246, 78 (1958).

/58/ Ray,G. and Ray,S.: Z. Krist. 122, 457 (1965).

/59/ International Tables for X-Ray Crystallography: Vol.I, p.314.
The Kynoch Press, Birmingham (1969).

/60/ James,R.W.: The Optical Principles of the Diffraction of X-Ray.
Bell,G. and Sons Ltd. London (1967).

/61/ Busing,W.R. and Levy,H.A.: Oak Ridge Report, ORNL-4054, Oak Ridge,
Tennessee (1967).

/62/ Patterson,A.L.: International Tables of X-Ray Crystallography,
Vol.II, p.61. The Kynoch Press, Birmingham (1972).

/63/ Rollett,J.S.: Computing Methods in Crystallography, pp. 22-23; 28-31
Oxford Pergamon (1965).

/64/ International Tables of X-Ray Crystallography: Vol.II, p.299.
The Kynoch Press, Birmingham (1972).

/65/ Weber,K.: Acta Cryst. B25, 1174 (1969).

/66/ Rouse,K.D. and Cooper,M.J.: Acta Cryst. A26, 682 (1970).

/67/ Zachariasen,W.H.: Acta Cryst. 16, 1139 (1963).

/68/ Cruickshank,D.W.: Computing Methods in Crystallography. Edited by Rollett,J.S. Oxford Pergamon, p.112 (1965).

/69/ Zwoll,K.: Berichte der Kernforschungsanlage Jülich, 1057-ZE (1974).

/70/ Zwoll,K. Müller,K. and Will,G.: Kerntechnik, 18, 435 (1976).

/71/ International Tables of X-Ray Crystallography, Vol.IV, p.71. The Kynoch Press, Birmingham (1974).

/72/ Prince,E. Dickens,B. and Rush,J.J.: Acta Cryst. B30, 1167 (1974).

/73/ Acarya,P.K. and Narayanan,P.S.: Proceedings of the nuclear and solid state physics symposium, India. 27-31, 152 (1973).

/74/ Copies may be obtained through Mineralogischen Institut der Universität Bonn, Poppelsdorfer Schloss, D-5300 Bonn, Federal Republic of Germany.